# Growth and characterization of ultrathin nitrided silicon oxide films

by E. P. Gusev H.-C. Lu E. L. Garfunkel T. Gustafsson M. L. Green

This paper reviews recent progress in understanding microstructural and growth-mechanistic aspects of ultrathin (<4 nm) oxynitride films for gate dielectric applications. Different techniques for characterizing these films are summarized. We discuss several nitridation methods, including thermal (oxy)nitridation in NO, N<sub>2</sub>O, and N<sub>2</sub> as well as a variety of deposition methods. We show that a basic understanding of the gas-phase and thin-film oxygen and nitrogen incorporation chemistries facilitates the processing of layered oxynitride nanostructures with desirable electrical properties.

#### 1. Introduction

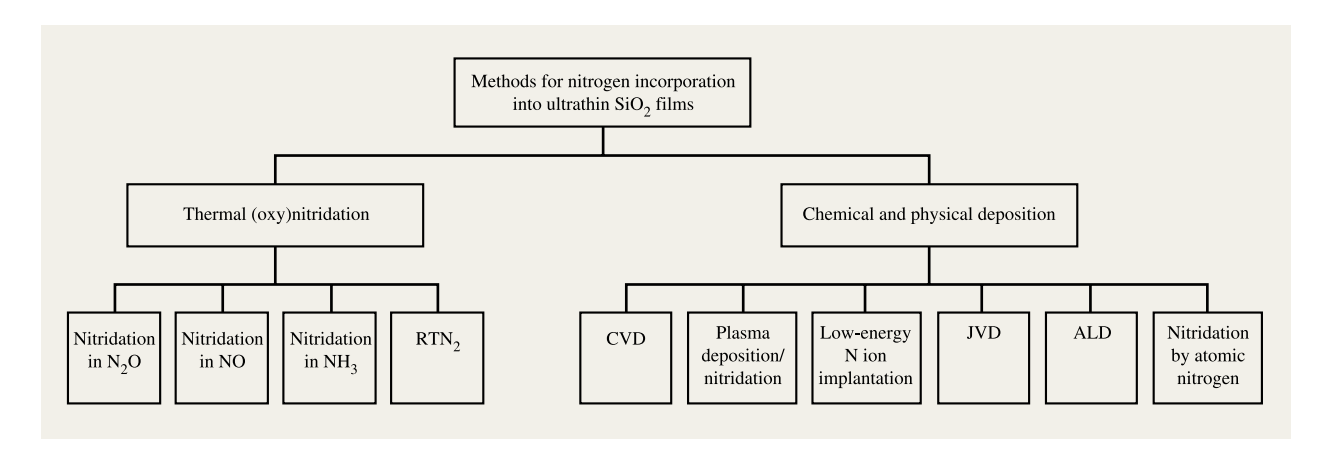
While "pure"  $SiO_2$  films remained the principal material for gate dielectrics in MIS-based structures for more than three decades, the use of the traditional  $SiO_2$  gate dielectric has become questionable for sub-0.25- $\mu$ m ULSI devices [1–5]. Increasing problems with dopant (boron) penetration through ultrathin  $SiO_2$  layers and direct tunneling for ultrathin (<2 nm) oxide films dictate the search for and aggressive exploration of new materials for future gate dielectric applications with better diffusion barrier properties and higher dielectric constants [6, 7]. At

this time, ultrathin silicon oxynitrides ( $SiO_xN_y$  or, more accurately, nitrogen-doped  $SiO_2$ ) are the leading candidates to replace pure  $SiO_2$  [8–24]. Oxynitrides exhibit several properties superior to those of conventional thermal  $O_2$  oxides ( $SiO_2$ ), the more important being suppression of boron penetration from the poly-Si gate and enhanced reliability. Nitrogen also reduces hot-electron-induced degradation [25]. The dielectric constant of the oxynitride increases linearly with the percentage of nitrogen from  $\varepsilon(SiO_2) = 3.8$  to  $\varepsilon(Si_3N_4) = 7.8$  [26, 27], though one should note that most  $SiO_xN_y$  films grown currently by thermal methods are lightly "doped" with N (<10 at.%) and therefore have a dielectric constant only slightly higher than that of pure  $SiO_3$ .

Recent publications suggest that the performance of CMOS-based devices depends on both the concentration and distribution of the nitrogen atoms incorporated into the gate dielectric [14, 16, 18, 28–30]. For example, excessive nitrogen at the interface may reduce peak carrier mobility in the channel of MOSFETs and may allow boron accumulation in the oxide, which, in turn, may result in device instabilities [28]. The optimal nitrogen profile is determined by its specific application, although our incomplete understanding of the atomic-scale structural and electronic properties of dielectrics makes the desired structure an imperfectly defined goal. One possibility is an SiO<sub>2</sub>N<sub>2</sub> film with two nitrogen-enhanced layers: first,

Copyright 1999 by International Business Machines Corporation. Copying in printed form for private use is permitted without payment of royalty provided that (1) each reproduction is done without alteration and (2) the Journal reference and IBM copyright notice are included on the first page. The title and abstract, but no other portions, of this paper may be copied or distributed royalty free without further permission by computer-based and other information-service systems. Permission to republish any other portion of this paper must be obtained from the Editor.

0018-8646/99/\$5.00 © 1999 IBM



Different nitridation methods.

nitrogen at or near the  $\mathrm{Si/SiO_2}$  interface to improve hot-electron immunity, and second, an even higher nitrogen concentration at the  $\mathrm{SiO_2/polysilicon}$  interface, as this is where it can best be used to minimize the penetration of boron from the heavily doped gate electrode [29]. The boron flux can be quite large (depending upon the thermal budget) and, therefore, higher nitrogen concentrations at the poly-Si interface are needed [28]. Although the actual "ideal" amounts of nitrogen required at each interface are not known, typical interfacial contents are of the order of  $(0.5-1)\times 10^{15}~\mathrm{cm^{-2}}$  near each interface. The best methods to produce the desired ultrathin  $\mathrm{SiO_xN_y}$  films are still under debate.

Nitrogen may be incorporated into SiO, using either thermal oxidation/annealing [8, 9, 12–14, 31–39] or chemical and physical deposition [15, 16, 18, 19, 40, 41] methods (Figure 1). Thermal nitridation of SiO, in NO or N<sub>2</sub>O generally results in a relatively low concentration of nitrogen in the films, of the order of 10<sup>15</sup> N/cm<sup>2</sup> [20, 29, 33, 42]. Since nitrogen content increases with temperature, thermal oxynitridation is typically performed at high temperatures, i.e., >800°C [20, 29, 33, 42]. For more heavily N-doped SiO<sub>x</sub>N<sub>y</sub> films, other deposition methods, such as chemical vapor deposition (CVD) [40] with different precursors and its low-pressure (LP) and/or rapid thermal (RT) variants [18], jet vapor deposition (JVD) [43], atomic layer deposition (ALD) [44], or nitridation by energetic nitrogen particles (plasma, N atoms, or ions) [45–55], can be used. These nitridation methods can be performed at lower temperatures, ~300-400°C. However, low-temperature deposition methods may result in nonequilibrium films, and subsequent thermal processing steps are often required to improve film quality and minimize defects and induced damage [19, 56]. Because

the thermodynamics [57, 58] of the SiO<sub>x</sub>N<sub>y</sub> system and the kinetics [12, 20, 29, 32, 38, 59–63] of nitrogen incorporation are rather complex, these different methods produce oxynitride films with different total nitrogen concentrations and depth distributions. From a scientific viewpoint, the addition of N into the Si–O system opens a number of questions concerning microstructure, defects, and growth mechanisms, issues which are still under intense debate even for the much simpler "pure" SiO<sub>2</sub>/Si system [64–71].

Characterizing the nitrogen distribution in ultrathin films with the required sub-nm accuracy is an analytical challenge. Conventional depth profiling approaches, such as SIMS (secondary ion mass spectroscopy) [9, 14, 18, 34, 72] and HF etch-back methods [12, 33, 35] [in combination with XPS (X-ray photoelectron spectroscopy), NRA (nuclear reaction analysis), etc.], offer limited depth resolution, especially for ultrathin dielectrics. In addition, SIMS analysis is complicated by matrix effects [73], while HF etching may introduce nonuniform oxide removal (especially in the presence of local nitrogen-rich regions) and other deleterious chemical effects. We have recently demonstrated [62, 63, 74-76] that high-resolution  $(\Delta E/E \approx 0.1\%)$  medium-energy ion scattering (MEIS) [77] is a useful technique for accurately obtaining the depth distribution profile of nitrogen in 1-4-nm oxynitride films with sub-nm accuracy.

In this paper, we review our recent progress in 1) characterizing nitrogen depth profiles (by MEIS [42, 74, 76]) and bonding (by XPS [78]) of ultrathin SiO<sub>x</sub>N<sub>y</sub> films, and 2) understanding the mechanisms of nitrogen incorporation into ultrathin oxide films [42, 62, 63, 79, 80]. We demonstrate how this basic knowledge can be used to guide nitrogen nanoengineering technology, in particular to

266

produce layered nitrogen structures [81]. A significant part of the paper is devoted to thermal oxynitridation of Si in NO and  $\rm N_2O$ . Other nitridation methods are also briefly discussed.

# 2. Thermodynamics of the Si-N-O system

The bulk phase diagram of the Si–N–O system is shown in **Figure 2**. The diagram consists of four phases: Si, SiO<sub>2</sub> (cristobolite, tridymite), Si<sub>3</sub>N<sub>4</sub>, and Si<sub>2</sub>N<sub>2</sub>O [57, 58]. The three compound phases have similar structural units: SiO<sub>4</sub> tetrahedra for SiO<sub>2</sub>, SiN<sub>4</sub> tetrahedra for Si<sub>3</sub>N<sub>4</sub>, and slightly distorted SiN<sub>3</sub>O tetrahedra for Si<sub>2</sub>N<sub>2</sub>O, implying that the phases can be converted from SiO<sub>2</sub> to Si<sub>2</sub>N<sub>2</sub>O and finally to Si<sub>3</sub>N<sub>4</sub> by replacing oxygen with nitrogen. However, the nitride (Si<sub>3</sub>N<sub>4</sub>) and the oxide (SiO<sub>2</sub>) phases never coexist in the bulk under equilibrium conditions. They are always separated by the oxynitride (Si<sub>2</sub>N<sub>2</sub>O), which is the only thermodynamically stable and crystalline form of silicon oxynitride.

A puzzling question is why nitrogen atoms are incorporated at all in  $\mathrm{SiO}_2$ . According to thermodynamic equilibrium, nitrogen should not incorporate into an  $\mathrm{SiO}_2$  film that is grown on Si in almost any partial pressure of oxygen, i.e.,  $>10^{-17}$  atm, depending upon temperature [57, 58]. One can see from Figure 2 that the  $\mathrm{Si}_2\mathrm{N}_2\mathrm{O/SiO}_2$  phase boundary exists at about  $10^{-18}$  atm for T=1400 K. At any oxygen partial pressure greater than that, which surely exists in a furnace or rapid thermal processing (RTP) reactor or, for example, during  $\mathrm{N}_2\mathrm{O}$  or NO decomposition at high temperatures, only  $\mathrm{SiO}_2$  phases (crystalline or amorphous) should form. Therefore, nitrogen in bulk  $\mathrm{SiO}_2$  is not thermodynamically stable.

At least two reasons for the presence of nitrogen in the SiO<sub>2</sub> film can be suggested. First, nitrogen atoms may simply be kinetically trapped at the reaction zone near the interface (i.e., the nitrogen is present in a nonequilibrium state, where the rate of the transition to equilibrium is slow and some N is trapped) or by structural defects in the SiO, film [82]. The basic idea in this model is that nitrogen brought into the film during oxynitridation (as, for example, NO; see below) reacts only with Si-Si bonds at or near the interface, not with Si-O bonds in the bulk of the SiO, overlayer. Alternatively, the nitrogen at the interface may indeed be thermodynamically stable due to the presence of free-energy terms that are not yet understood. For example, nitrogen may lower the interfacial strain known to exist at the SiO<sub>2</sub>/Si interface. This could explain why incorporated nitrogen (especially in N<sub>2</sub>O or NO oxides) is often associated with the Si/SiO<sub>2</sub> interface, consistent with a special, stabilizing role of the nitrogen at the interface. Even when nitrogen is implanted into Si, it tends to migrate to the Si/SiO, interface during oxidation and be incorporated in the SiO, [83, 84]. Therefore, there is some evidence that the nitrogen

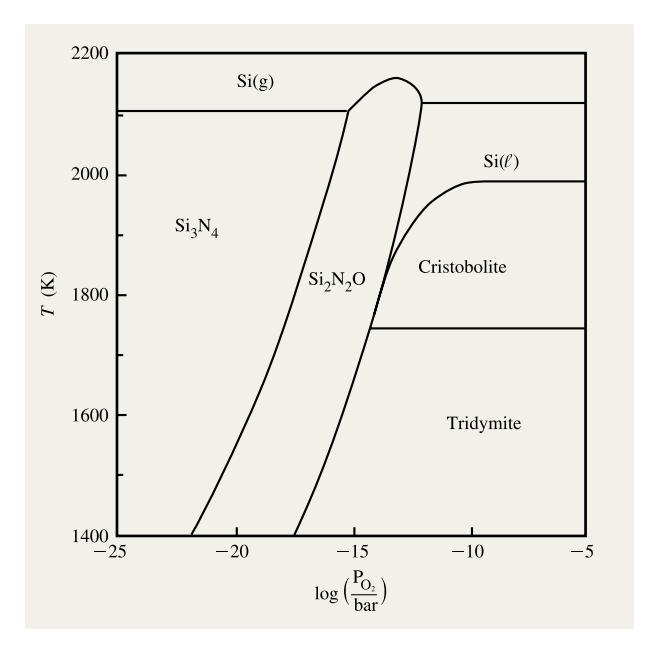


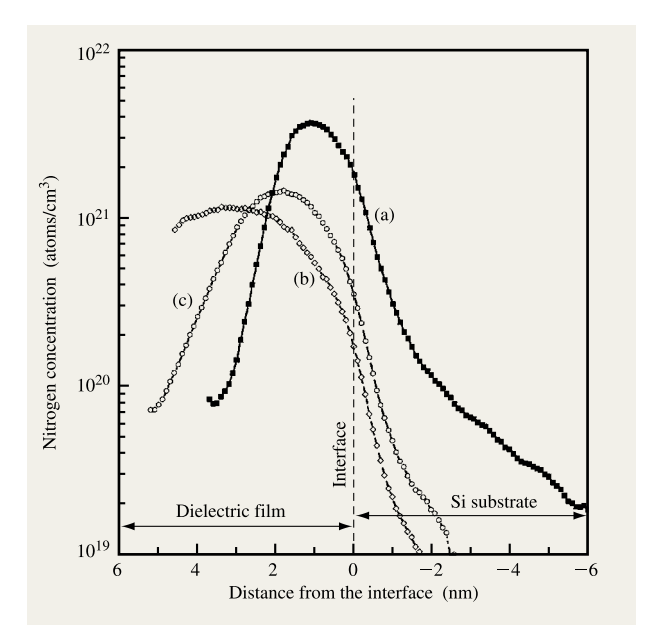
Figure 2

Thermodynamic phase diagram of the Si–N–O system (after [29, 58], with permission).

plays a specific role at the interface, but also that it is not stable away from it. On the other hand, nonequilibrium techniques (for example, plasma nitridation) have yielded oxynitrides with much higher concentrations of incorporated nitrogen (including top-surface nitridation [49]) than thermal oxynitridation methods (e.g., in NO,  $N_2O$ ,  $N_2$ ). This fact seems to be supportive of the "kinetic trapping" concept. Finally, we note that the favorable thermodynamics of the  $SiO_2$  phase discussed above may be the reason why  $Si_3N_4$  films (produced by JVD or other methods) always contain some oxygen; of course, contamination by  $H_2O$ ,  $O_2$ , etc. with a high sticking coefficient would also result in mixed oxide–nitride phases.

# 3. Diffusion-barrier properties of nitrided layers

An important property of nitrogen in nitrided oxides is that it forms a barrier against the diffusion of boron. Concurrent with this, it also lowers the diffusion rates for oxygen, nitric oxide, and other dopants, significantly slowing the rate of further oxidation or nitridation [21, 32, 34, 63, 82, 85–90]. For example, for a 2-nm oxynitride with ~1 ML (monolayer) of nitrogen (6.8 × 10<sup>14</sup> N/cm²) located near the interface, the rate of continued oxidation at 900°C decreases by at least a factor of 4 relative to the pure oxide. A reasonable argument can be made that the decrease in film growth rate (due to nitrogen) results from



Nitrogen depth profiles obtained by SIMS (Evans East) for (a) 4.5-nm  $SiO_2$  film annealed in NO at 950°C for one hour; (b) film grown in  $N_2O$  in a furnace at 850°C for 110 min; and (c) oxynitride film grown by RTP in  $N_2O$  at 1000°C for 2.3 min (after [74], with permission).

a decreased rate of diffusion. The density of nitrides and oxynitrides is higher than that of the pure oxide [40]; thus, the diffusivity of NO, O2, N2, or other nonreactive molecular species such as noble gases should be lower in the nitrogen-containing films. However, another property involving N bonds may be equally important: The lattice itself may become more rigid on an atomic level. The three bonds connected to each nitrogen (as in Si<sub>2</sub>N<sub>4</sub>) are more constrained than the two bonds of each O atom in SiO<sub>2</sub>, where the Si-O-Si bond angles can go from 120° to 180° with little change in energy; this may also contribute to a decrease in the ability of the nitrided lattice to permit diffusion of atoms and small molecules. The latter argument is valid for either an interstitial diffusion mode (of molecules), or an exchange-hopping substitutional mode (of excess atoms).

By analogy, both physical (e.g., density) and chemical arguments have been used to explain the important effect of the reduced penetration rate of boron from the poly-Si gate into nitrided oxides. (Boron penetration causes threshold voltage shifts and degrades reliability.) To explain the "stopping power" of the nitrogen in oxides, a model assuming boron diffusion via peroxy linkage defects (Si-O-O-Si bonds), whose concentration changes under different processing conditions and film thicknesses, has

been suggested [91]. For a 1.5-nm SiO<sub>2</sub> film, the diffusivity at 900°C would increase by a factor of 24 as compared with 10-nm oxides. According to this model, the role of nitrogen is that the N atoms compete with B for occupation of the defect sites. The model was criticized by Ellis and Buhrman [92], who argued that 1) Si-O-N-O-Si structures, which should form after N passivation, are not observed in XPS; and 2) according to percolation theory, to fit the experimental data the peroxy defects should have an unreasonably high concentration (~40% of the Si-O-Si bonds). Ellis and Buhrman developed a model in which boron diffuses substitutionally for Si atoms, and the role of the Si-N bond is to impede substitution for that Si atom [92]. The model was incorporated into a Monte Carlo simulation and showed good agreement with experimental data.

Another interesting aspect of the diffusion barrier property of nitrided layers is that silicon interstitials generated during the film growth reaction at the interface are blocked from diffusing into the oxide [93]. This results in an enhanced flux of the interstitials into the Si substrate, which in turn yields an increased density of oxidation stacking faults and may also affect oxidationinduced diffusion [93]. Finally, we note that other chemistries may play an important role both in film growth processes and in the more technically important issue, electrical defects that occur in the final devices. Hydrogen, water, and various other species quite possibly exist at finite concentrations [94]. For example, both fluorine and hydrogen enhance the boron diffusion rate [91]. Hydrogen may also play an important role in the diffusion/reaction processes during (oxy)nitride formation [40].

# 4. Materials characterization of ultrathin nitrided oxides

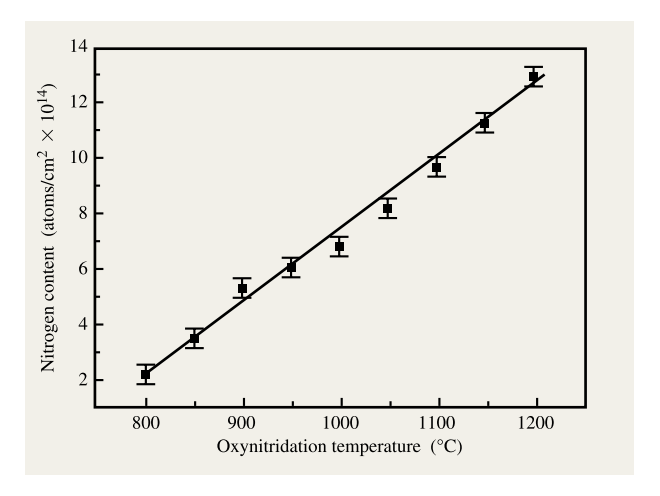
Two major problems in measuring nitrogen in SiO<sub>2</sub>N<sub>2</sub> films are the following: 1) In many cases the concentration of nitrogen in the film is rather low (as an example, in earlier studies of NO oxynitrides [95] it was claimed that the films are essentially SiO<sub>2</sub> because the nitrogen was undetectable at that time); and 2) the films in question are very thin (<5 nm), suggesting that sub-nm depth resolution is required to monitor nitrogen depth profiles. Over the past few years, several techniques, such as secondary ion mass spectroscopy (SIMS) [18, 34, 72, 73, 78], nuclear reaction analysis (NRA) [29, 32, 33, 38, 59, 80, 96, 97], mediumenergy ion scattering (MEIS) [39, 42, 62, 63, 74–76, 80], X-ray photoelectron spectroscopy (XPS) [12, 30, 34, 35, 37, 48, 74, 78, 87, 98–101], Auger electron spectroscopy (AES) [19], Fourier transform infrared spectroscopy (FTIR) [102], spectroscopic ellipsometry [103], and others have been utilized to study nitrogen concentrations, depth profiles, nitrogen bonding, and microstructure of

 Table 1
 Selected nuclear reactions for oxynitride characterization.

Target element	Nuclear reaction	Energy (keV)	Sensitivity (atoms/cm <sup>2</sup> )
Н	$H(^{15}N, \alpha\gamma)^{12}C$	6420	$\sim \! 10^{14}$
D	$D(^{3}He, p)^{4}He$	700	$\sim \! 10^{12}$
$^{14}N$	$^{14}N(d, \alpha_{0,1})^{12}C$	1100	$\sim$ 5 × 10 <sup>13</sup>
$^{15}N$	$^{15}N(p, \alpha)^{12}C$	1000	$\sim \! 10^{12}$
$^{15}N$	$^{15}N(p, \alpha\gamma)^{12}C$	429	$\sim \! 10^{13}$
			(estimated)
<sup>16</sup> O	$^{16}O(d, p)^{17}O$	850	$\sim \! 10^{14}$
<sup>18</sup> O	$^{18}{\rm O}({\rm p},~\alpha)^{15}{\rm N}$	730	$\sim \! 10^{12}$
$^{18}O$	$^{18}{\rm O(p,\ }\alpha)^{15}{\rm N}$	151	$\sim \! 10^{13}$
			(estimated)
<sup>28</sup> Si	$^{28}$ Si(p, $\gamma$ ) $^{29}$ P	371	
<sup>29</sup> Si	$^{29}$ Si(p, $\gamma$ ) $^{30}$ P	324	$\sim \! 10^{13}$
	,	417	(estimated)
<sup>30</sup> Si	$^{30}$ Si $(p, \gamma)^{31}$ P	499	$\sim 10^{13}$ (estimated)

oxynitrided films. Below we outline the features and the utility of these techniques for ultrathin oxynitride studies.

SIMS, a standard technique used in the industry to monitor concentration profiles in semiconductor structures, was one of the first methods applied to the nitrogen depth distribution problem in oxynitrided films. The technique has a rather high sensitivity (of the order of 0.001 at.%), can be performed rapidly, and shows good long-term reproducibility [73]. As an example, Figure 3 illustrates nitrogen depth profiles for ~5-nm oxynitride films grown by thermal oxynitridation of Si(100) in N<sub>2</sub>O (both in a furnace and in an RTP reactor), and in O<sub>2</sub> followed by NO [74]. One can see different depth profiles depending on the processing conditions. The NO-annealed film has the highest concentration of nitrogen incorporated near the SiO<sub>2</sub>N<sub>2</sub>/Si interface. The RTN<sub>2</sub>O (rapid thermal oxynitridation) film also shows nitrogen located near the interface, whereas the furnacegrown film has a broader nitrogen depth distribution. Both N<sub>2</sub>O oxynitrides have nitrogen concentrations lower than the NO-annealed film. The technique begins to reach the limits of depth resolution (estimated to be  $\sim 2-3$  nm) for sub-5-nm films. Another more important complication for SIMS analysis are "matrix effects," in which the sputtered nitrogen ion yield depends strongly on the local film chemistry around the nitrogen. For example, the (CsN<sup>+</sup>) ion yield from nitrogen in bulk Si is about six times smaller than in SiO<sub>2</sub>, while that for N near the interface is about three times that observed in the bulk of the SiO, film [73]. The use of CsN<sup>+</sup> ions as the detected species

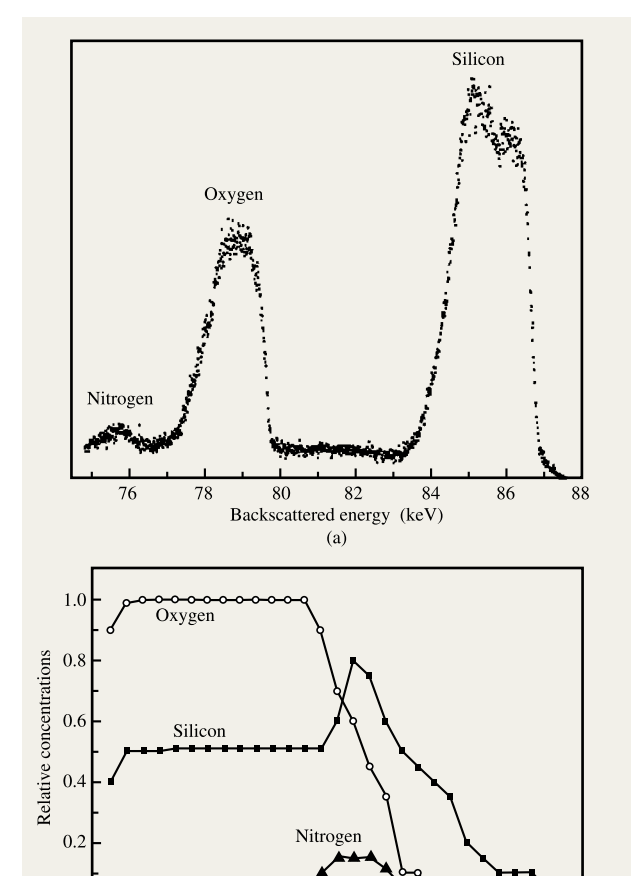


#### Figure 4

Nitrogen content in 10-nm oxynitride films grown in  $N_2O$  by RTP, as measured by NRA (after [33]).

seems to minimize the matrix effect, since for negative ions matrix effects are even more severe. In most cases, SIMS analysis is also complicated by surface contamination and initial sputtering effects which make measurements of the nitrogen in the top (~1 nm) surface layers not very meaningful. Finally, one more metrological aspect of the SIMS analysis is that the N concentration shown for the interface peak (see Figure 3) may not be accurate due to ion mixing. The areal density of the N peak should be used instead. Reference samples (especially with different nitrogen distributions) calibrated by other quantitative methods (NRA, MEIS, etc.) may be helpful for more accurate quantitative SIMS analysis.

NRA analysis of oxynitrides is based on the detection of protons,  $\alpha$ -particles, and  $\gamma$ -rays generated in nuclear reactions of nitrogen, oxygen, silicon, and hydrogen (deuterium) induced by high-energy charged particles (**Table 1**) [29, 32, 33, 38, 59, 80, 96, 97]. The cross sections for these reactions can be determined in independent calibration experiments, and the signal-to-background ratio is in many cases quite favorable. Since the nuclear reaction rates are sensitive only to the number of nuclei in the films, the technique yields absolute concentrations of the species investigated. In particular, the technique allows one to determine the absolute concentration of <sup>14</sup>N with an accuracy of  $\sim$ 7-10% and a detection limit of  $\sim 5 \times 10^{13}$  atoms/cm<sup>2</sup> via the reaction of  $^{14}$ N(d,  $\alpha_{0.1}$ ) $^{12}$ C induced by 1.1-MeV deuterons. Figure 4 shows the nitrogen content (which is an increasing function of temperature) in oxynitride films grown by rapid thermal oxynitridation in N<sub>2</sub>O [33]. The oxygen content in the films can also be measured by NRA, for example by the  ${}^{16}O(d, p){}^{17}O$ 



(a) MEIS spectrum for a 4.5-nm  ${\rm SiO_2}$  film annealed in NO at 950°C for one hour. Primary energy of the proton beam is 97.2 keV. The spectrum is taken in a channeling direction. Scattering angle is 125°. Corresponding oxygen, silicon, and nitrogen depth profiles are shown in part (b).

Distance from the outer surface (nm)

reaction at 850 keV. This allows one to calculate the thickness of the films (provided that film density is known). An additional advantage of the NRA technique is the detection of nitrogen ( $^{15}$ N) and oxygen ( $^{18}$ O) isotopes with the help of the following reactions:  $^{15}$ N(p,  $\alpha$ ) $^{12}$ C at 1000 keV,  $^{18}$ O(p,  $\alpha$ ) $^{15}$ N at 730 keV, and the resonant reactions of  $^{15}$ N(p,  $\alpha\gamma$ ) $^{12}$ C at 429 keV and  $^{18}$ O(p,  $\alpha$ ) $^{15}$ N at 151 keV. Isotopic labeling has been proven to be a useful method to study mechanistic aspects (including nitrogen and oxygen transport) of silicon (oxy)nitridation [38, 59, 97, 104]. Owing to the narrow resonances (with widths of 120 and 100 eV, respectively), the latter two reactions can be used for depth profiling of  $^{15}$ N and  $^{18}$ O on an

approximately 1-nm scale under favorable conditions. Depth profiling can also be performed by an HF acid etch-back with subsequent NRA measurement of N remaining in the film [13]. One more useful application of NRA is based on its ability to measure hydrogen/deuterium [H( $^{15}$ N,  $\alpha\gamma$ )) $^{12}$ C at 429 keV and D( $^{3}$ He, p) $^{4}$ He at 700 keV] since H/D is believed to be important in both the nitridation mechanism and device performance [105, 106]. Finally, we note that nitrogen, oxygen, silicon, and hydrogen can also be monitored by the technique of elastic recoil detection (ERD) of primary MeV ions [86].

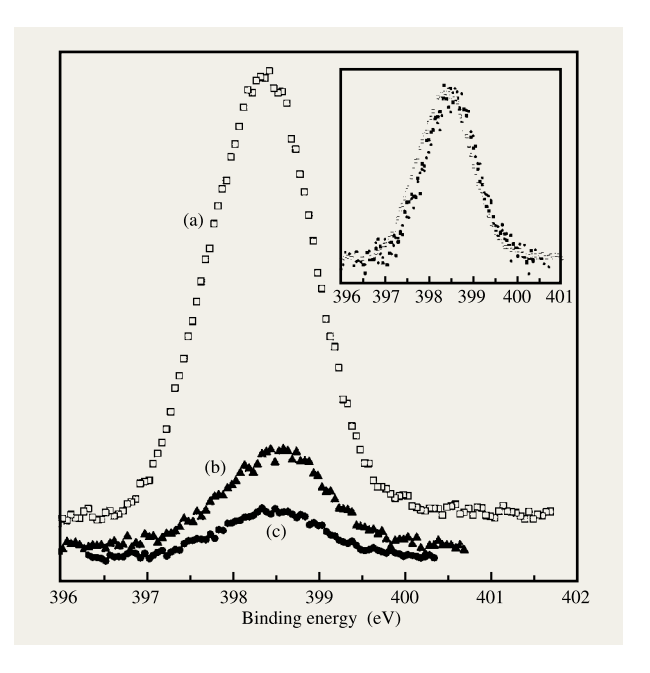
MEIS, another ion beam technique, is based on the same principles of ion-solid interactions as is conventional Rutherford backscattering spectroscopy (RBS) [77]. Because of the lower ion energy used in MEIS (typically 100 keV, at which the energy loss of protons in a solid is maximal), and the use of a highresolution toroidal electrostatic ion energy analyzer [107]  $(\Delta E/E \approx 0.1\%)$ , almost-monolayer depth resolution can be obtained [108, 109]. We have demonstrated that a 0.3-0.5-nm accuracy (near the top surface or for very thin films) in the nitrogen depth profiles can be achieved [42, 74]. To our knowledge, this is the best depth resolution for nitrogen in SiO<sub>2</sub>N<sub>2</sub> films achieved so far. However, due to the statistical nature of the ion energy loss in the solid (straggling effect) [110], the resolution decreases with increasing distance from the surface. MEIS allows one to monitor simultaneously both absolute concentrations and depth profiles of N, O, and Si in the film. The detection limit of nitrogen in SiO<sub>2</sub> is about  $2-3 \times 10^{14}$ atoms/cm<sup>2</sup>, depending on the film thickness and the width of the nitrogen distribution in the film. It is worth noting that, in opposition to other depth-profiling techniques (e.g., SIMS), both the sensitivity to nitrogen and the depth resolution increase with decreasing dielectric film thickness. Another strength of MEIS is mass sensitivity, which enables isotopic (<sup>18</sup>O and <sup>16</sup>O) labeling experiments [111, 112]. Light elements (for example, hydrogen and boron) can also be detected in the elastic recoil configuration, as demonstrated by Copel and Tromp [113, 114].

Figure 5(a) shows a typical MEIS spectrum for an SiO<sub>2</sub> film annealed in NO. Three peaks are seen in this spectrum, corresponding to nitrogen, oxygen, and silicon. The lighter mass (nitrogen) yields a peak at lower energy, as given by classical two-body scattering kinematics [77]. The areas under the peaks (after corrections for the known cross sections) are proportional to the total amounts of oxygen and nitrogen in the film [77]. Obviously, the amount of nitrogen is much smaller than that of oxygen. The shape of the nitrogen peak is determined by the depth distribution of nitrogen in the film. Because of energy loss arising from electronic

excitations, protons backscattered from nitrogen atoms closer to the  $\operatorname{Si-SiO}_x \operatorname{N}_y$  interface have lower energy than those scattered off the atoms near the surface. Accurate depth distributions [**Figure 5(b)**] of Si, O, and N are deduced from simulations of energy spectra, as discussed in [111]. More details about the MEIS setup, data acquisition and analysis, and the isotopic labeling technique can be found elsewhere [74, 108, 111, 112, 115–117].

The above ion beam methods are unfortunately not capable of examining local nitrogen bonding in (oxy)nitrided films. Photoemission (XPS) is a common technique used to help determine local bonding configurations of atoms on a surface or in a thin film [68, 118-121]. XPS analysis is based on the fact that the energies of the electronic core levels are altered by the local electronic configurations. The observed energy levels shift with changing local chemical environment (the so-called chemical shifts). Early XPS studies were limited to the detection of nitrogen at the interface of SiO, annealed in nitrogen [87, 98]. More recent high-resolution (including synchrotron-based) photoemission studies of core levels of nitrogen (N 1s) and silicon (Si 2p) atoms were useful in understanding nitrogen bonding and depth distribution (with HF etch-back or variable photoelectron takeoff angle methods) [35, 37, 78, 99, 122]. Depth analysis in XPS is determined by the escape depth of the N 1s or Si 2p photoelectrons, which are of the order of 2-3.5 nm for conventional AlK or MgK X-ray sources. N 1s spectra for NO and N<sub>2</sub>O oxynitrides are shown in Figure 6 [78]. The nitrogen spectrum for the N<sub>2</sub>O-grown film has much lower intensity than that of the NO oxynitride, which indicates that an NO source is more effective in terms of nitrogen incorporation into the dielectric film. A second feature to point out is that the spectra for both NO and N<sub>2</sub>O oxynitrides have similar shapes (see inset), suggesting that the local bonding configurations of nitrogen in the two films are similar.

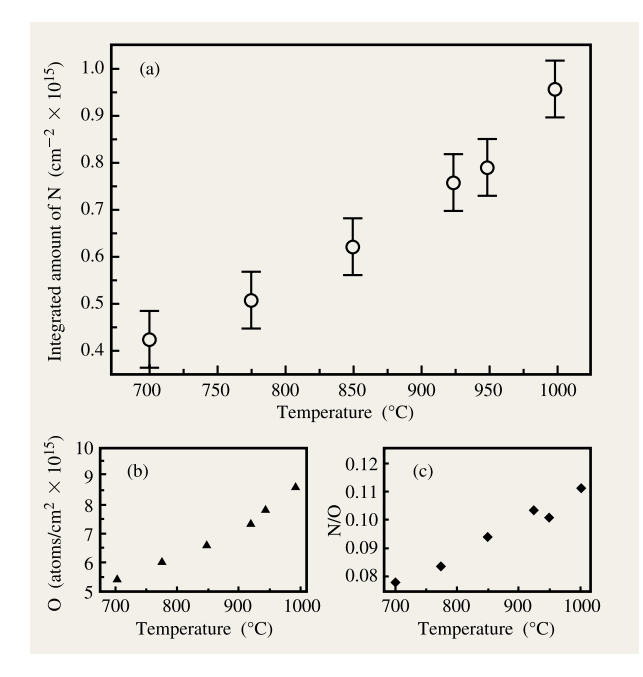
A more detailed analysis of the N 1s peak shape shows that the peak is asymmetric and consists of at least two components [35, 78, 99]. The lower binding energy (BE) component at ~397.6 eV (calibrated with respect to the Si 2p peak at 99.2 eV) is located closer to the interface, while the higher BE component at 398.3-399.0 eV (the thicker the film, the higher the value) corresponds to nitrogen atoms located further into the overlayer film. The lower BE peak can be assigned to N atoms bonded to three Si atoms, as follows from the observation of an N 1s peak at ~397.6 eV from a reference Si<sub>3</sub>N<sub>4</sub> film [35, 99]. The shift of the higher BE component originates from both electrostatic (charging, core hole screening) and structural effects. The structural effects may include different bond length and bond angles in the "bulk" of the film and near the interface, strain near the interface,



## Figure 6

N 1s XPS spectra for (a)  $\sim$ 2.5-nm oxynitride film grown in NO at 1000°C; (b)  $\sim$ 6-nm (as grown at 1000°C) RTN<sub>2</sub>O film; and (c) the same film HF-etched back to  $\sim$ 3 nm. The inset shows the same spectra normalized to the same maximum intensity (after [78]).

and/or second-neighbor effects (i.e., bonding/atoms in the shell of second neighbors near the interface may be different from those in the middle of the oxynitride film) [100]. N-O bonds are unlikely to be present at high concentration in the NO and N<sub>2</sub>O oxynitrides because the chemical shift of  $\sim 1.5$  eV (relative to the N-Si bond) calculated recently [100] for this configuration is larger than any experimentally observed ones. Recent work by R. Opila and J. Chang demonstrated that nitrogen profiles obtained from angular resolved XPS were consistent with MEIS depth profiles. They also showed that for oxynitride films processed by plasma, metastable nitrogen states may be observed with binding energies greater than 400 eV. Finally, we note that XPS is also useful in obtaining film thickness [123] (from the ratio of Si 2p peaks corresponding to the film and Si substrate) and interface structure [30, 35, 68, 118, 121, 124] (from the concentration of Si<sup>1+</sup>, Si<sup>2+</sup>, and Si<sup>3+</sup> suboxide states observed in the Si 2p spectrum). Recent XPS studies of the suboxide states in N<sub>2</sub>O oxynitrides were interpreted as giving evidence for a lower defect density at the SiO<sub>2</sub>N<sub>2</sub>/Si interface with respect to the SiO<sub>2</sub>/Si interface [35]. However, an opposite effect (i.e., an increased concentration of the Si1+ state and an unchanged concentration of the Si<sup>1+</sup> and Si<sup>2+</sup>) has also been reported



Concentrations of (a) nitrogen and (b) oxygen, and (c) nitrogen-to-oxygen ratio in ultrathin  $SiO_x N_y$  films grown in NO, as measured by MEIS (after [42], with permission).

[30]. Another electron spectroscopy, AES, can also be used to measure nitrogen content in  $SiO_xN_y$  films and has been used effectively in studies of plasma-nitrided samples [19]. Though the AES sensitivity to nitrogen is similar to that of XPS, the interpretation of spectral features is usually more difficult than in XPS because the Auger electron emission process is more complex than photoemission.

Finally we discuss some other techniques for characterizing nitrogen and SiO<sub>x</sub>N<sub>x</sub> film microstructure. The amount of nitrogen can be crudely estimated from oxidation kinetics measurements. Since nitrogen significantly retards transport/reactions in (oxy)nitrided films [32, 34], this simple method can be used to monitor the presence of nitrogen in the film and to compare its relative value in different samples. However, the retardation rate depends not only on the N concentration but also on the depth distribution. A given amount of N evenly distributed in the film would produce a diffusion barrier quite different from one in which the nitrogen distribution is sharply peaked, making quantitative analysis difficult. Spectroscopic (immersion) ellipsometry results on N<sub>2</sub>O- and NO-grown oxynitrides show an agreement with SIMS measurements, though one should keep in mind that ellipsometric analysis is very dependent on parameters

and models [103]. A structural two-layer model of  $N_2O$  oxynitride films with an  $\sim 1.4$ –1.6-nm-thick  $Si_2N_2O$  phase near the interface was suggested to explain a shift of the main peak in the FTIR spectrum as a function of the thickness of the films [102]. Optical second-harmonic spectroscopy has been used to study strain at the interface [125, 126]. Roughness at the  $SiO_xN_y/Si$  interface was studied by X-ray diffraction. It was found that, for  $N_2O$  oxynitrides, the (RMS) roughness is smaller than for pure  $SiO_2$  films and decreases with temperature [33].

# 5. Thermal (oxy)nitridation methods

• Nitrogen incorporation into ultrathin dielectrics by NO processing

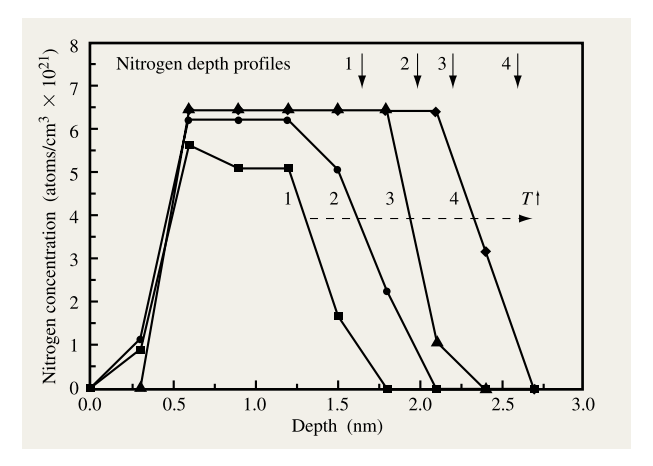
Oxidation of silicon and annealing of SiO2 in nitrous (N<sub>2</sub>O) or nitric (NO) oxides are the leading hydrogenfree processing methods for making nitrided oxides by conventional thermal routes [20, 21, 29]. Oxynitridation in N<sub>2</sub>O is particularly attractive because 1) it allows one to incorporate what appears to be an appropriate amount of nitrogen near the SiO<sub>x</sub>N<sub>x</sub>/Si interface (typically  $\sim 5 \times 10^{14}$ atoms/cm<sup>2</sup>); and 2) its processing similarity to O<sub>2</sub> permits N<sub>2</sub>O to replace oxygen in oxidation reactors/furnaces. However, among other factors, oxynitridation in N<sub>2</sub>O is complicated by the fast gas-phase decomposition of the molecule into N<sub>2</sub>, O<sub>2</sub>, NO, and O at typical oxidation temperatures, 800-1100°C (see the subsection on gasphase N<sub>2</sub>O decomposition which follows). NO is now believed to be responsible for nitrogen incorporation into the film [21, 29, 31, 37, 60, 127, 128], suggesting that understanding oxynitridation in NO is a necessary step before considering more complex gases such as N<sub>2</sub>O. If NO is the main species responsible for nitrogen incorporation into the film, oxynitridation in pure NO should be considered for ultrathin dielectrics, especially in processes in which thermal budget and film thickness issues are crucial. Compared to N2O, oxynitridation in NO results in more nitrogen incorporation at equivalent temperatures [14, 34, 37, 74, 82]. In addition, NO oxynitrides exhibit lower leakage currents and interface defect densities, as well as improved electrical stress properties [14, 34]. However, channel mobility may be reduced if the nitrogen concentration near the interface is too high.

Figure 7 shows the total amounts of oxygen and nitrogen in ultrathin films on Si(100) after exposure in NO for an hour in the temperature range of  $700-1000^{\circ}C$  [42]. As the temperature increases, the total amounts of both nitrogen and oxygen increase. One should also note that the ratio of nitrogen to oxygen in the film increases with increasing temperature (increasing by  $\sim 50\%$  from 700 to  $1000^{\circ}C$ ). This was also observed during the initial stage of the interaction of NO with Si(111) at much lower pressure

 $(10^{-6}\ \text{Torr})$  [129]. In other words, the film becomes more nitride-like at higher temperatures. The fact that the concentration of nitrogen increases with temperature has an important implication for the (oxy)nitridation of silicon in N<sub>2</sub>O. It was observed that in the case of N<sub>2</sub>O, a higher (oxy)nitridation temperature also gives rise to a higher nitrogen content in the film (Figure 4); this was attributed to a higher percentage of NO in the product stream resulting from the N<sub>2</sub>O gas-phase decomposition at higher temperatures. Our results with NO as the only reactive gas clearly show that the solid-state chemistry is also important in the understanding of the incorporation and distribution of nitrogen in the dielectric layer.

Quantitative MEIS nitrogen depth profiles corresponding to NO oxynitrides grown at different temperatures are shown in Figure 8 [42]. The width of the nitrogen-containing region increases with temperature. As the position of the interface (deduced from the oxygen depth profile and marked by arrows) propagates deeper into the Si substrate with increasing temperature, the nitrogen follows the movement of the interface such that, for the samples we examined, the nitrogen is distributed almost evenly in the films (also observed in a recent XPS/Ar<sup>+</sup> sputtering depth profiling study [37]), except for the very near-surface SiO, region. These results are inconsistent with a model of a (continuous) single silicon nitride (Si<sub>3</sub>N<sub>4</sub>) layer near the interface. We further note that while recent SIMS results [34] on silicon (furnace) nitridation in NO were interpreted in terms of a nitrogen distribution sharply peaked on the substrate (silicon) side of the interface, rather than in the near-interfacial oxide, our MEIS studies did not find any evidence of significant nitrogen incorporation into the substrate. In addition, multiple features in angularly dependent core-level (N 1s and Si 2p) photoemission [34, 35, 74] and the multiphase nature of EPR signals from oxynitrides [130] suggest more complex (other than a single Si<sub>3</sub>N<sub>4</sub> phase) local chemical bonding in the film.

Owing to the relatively high concentration of nitrogen incorporated into NO films, the kinetics of reoxynitridation are very slow. (The role of nitrogen in retarding the oxidation rate is discussed by us [32, 63] and by others [87, 88] elsewhere.) The thicknesses of the films after clean silicon surface exposure at 700-1000°C for one hour were only  $\sim$ 1.5–2.5 nm (Figure 8), consistent with earlier kinetic studies [95]. From a practical viewpoint, the slower growth of the oxynitride compared to a pure oxide facilitates good thickness control in the ultrathin regime during high-temperature processing. To make a thicker film, a thin preoxide (SiO<sub>2</sub>) of desired thickness can first be formed, followed by an NO anneal. Typically NOannealed preoxides yield nitrogen distributions different from the NO-grown films; that is, the nitrogen becomes concentrated near the interface [Figure 5(b)]. The kinetics



#### Figure 8

Nitrogen MEIS depth profiles (as a function of the distance from the outer surface) for oxynitride films grown in NO at 700°C (1), 850°C (2), 925°C (3), and 1000°C (4). The arrows show interface position for each film (after [42]).

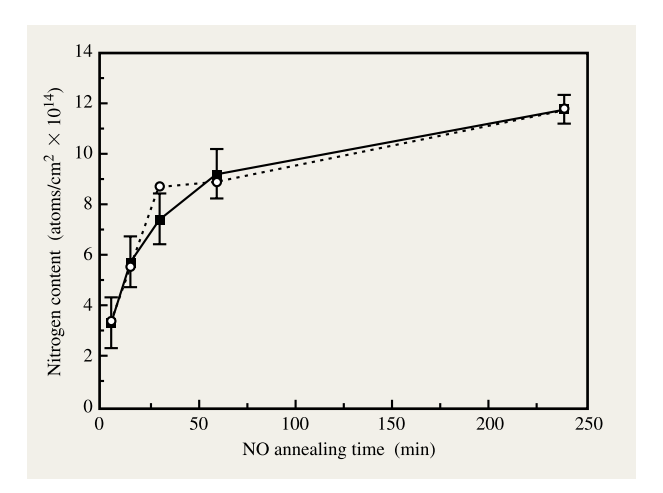
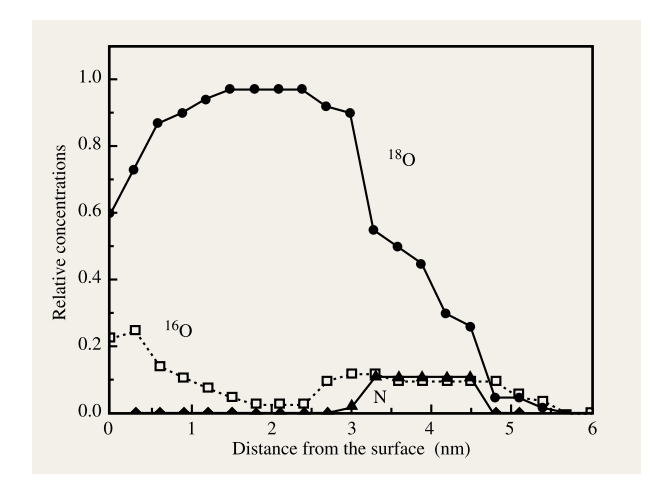


#### Figure 9

Kinetics of nitrogen accumulation in a 4.5-nm preoxide annealed in NO at 850°C. The solid symbols represent the data obtained by MEIS; open symbols show NRA results.

of nitrogen accumulation in a 4.5-nm  $\mathrm{SiO}_2$  film annealed in NO at 850°C is shown in **Figure 9**. One can see that after a fast initial accumulation, the rate of nitrogen incorporation becomes much slower at >60 min. Also noteworthy is that the total concentration of nitrogen for an NO-annealed preoxide is comparable to the concentration of an NO-grown film oxidized under equivalent conditions, at least for long oxynitridation times (cf. Figure 7).



Isotopic labeling of the silicon oxynitridation in NO. The <sup>18</sup>O (solid circles), <sup>16</sup>O (open squares), and N (solid triangles) depth profiles are obtained for an Si<sup>18</sup>O<sub>2</sub> film annealed in N<sup>16</sup>O.

**Table 2** Reaction scheme for N<sub>2</sub>O decomposition.

1.	$N_2O \rightarrow N_2 + O$
2.	$N_2O + O \rightarrow NO + NO$
3.	$N_2O + O \rightarrow N_2 + O_2$
4.	$O + O \rightarrow O_2$
5.	$\mathrm{NO}+\mathrm{O}\rightarrow\mathrm{NO}_{2}$
6.	$NO_2 + O \rightarrow NO + O_2$
7.	$NO_2 + NO_2 \rightarrow NO + NO + O_2$
8.	$NO_2 \rightarrow NO + O$
9.	$NO_2 + NO_2 \rightarrow NO_3 + NO$
10.	$NO_3 + NO \rightarrow NO_2 + NO_2$
11.	$NO_2 + O \rightarrow NO_3$
12.	$NO_3 \rightarrow NO + O_2$
13.	$NO_3 + O \rightarrow O_2 + NO_2$
14.	$NO_2 + NO_2 \rightarrow N_2O_4$
15.	$N_2O_4 \rightarrow NO_2 + NO_2$
16.	$NO_2 + NO_3 \rightarrow N_2O_5$
17.	$N_2O_5 \rightarrow NO_2 + NO_3$
18.	$O_2 + O \rightarrow O_3$
19.	$O_3 \rightarrow O_2 + O$
20.	$O_3 + O \rightarrow O_2 + O_2$
21.	$O_3 + NO \rightarrow NO_2 + O_2$

The N pileup near the interface for the NO-annealed preoxides implies that the dominant transport during NO oxynitridation is NO molecular diffusion to the interface. To verify this idea with isotopic labeling, in Figure 10 we present results of the reaction of an Si18O2 film, oxidized initially with <sup>18</sup>O<sub>2</sub>, that is further reacted with N<sup>16</sup>O. It is evident that the N and <sup>16</sup>O yields near the SiO<sub>2</sub>N<sub>2</sub>/Si interface overlap (centered at 4 nm below the surface). The classic Deal-Grove model [131] of silicon oxidation argues that SiO, film growth occurs by neutral molecular oxygen diffusing through the SiO, film and reacting at the SiO<sub>2</sub>/Si interface. We [75, 111, 116, 117] and others [132–134] have refined the model, pointing out the existence of rather complex surface and near-interface (SiO<sub>2</sub>/Si) reactions; however, the basic tenet of molecular O<sub>2</sub> diffusion still holds (at least for films >1.5 nm). No equivalent "standard" model for N incorporation during oxynitride growth exists. Two likely candidates to explain N incorporation are 1) direct N atom addition at the surface (from N<sub>2</sub>O, NO, or N atoms present in the gas phase), and 2) NO diffusion to and reaction in the nearinterfacial region, analogous to O, in the Deal-Grove model. If N or O atoms were present at the outer surface and diffused from the surface to the near-interface region, it is unlikely that both would pass atomically through the film without exchanging with lattice oxygen. The energy of an isolated, noninteracting interstitial N or O atom is very high and can be immediately lowered by insertion into an Si-Si, Si-N, or even Si-O bond. Although O is relatively more stable than N in an oxynitride, both O and N atoms should bond immediately to the lattice when present as isolated species inside the film. Isolated N or O atoms introduced at the surface should prefer to incorporate mostly at the surface, with a long tail decaying into the film. Since both N (and an equivalent or greater amount of O) atoms incorporate into the films with similar depth distributions (Figure 10), we propose that NO diffuses molecularly into the SiO, lattice (analogous to O, in the Deal-Grove model [131]). We further argue that NO should dissociate when it encounters unoxidized or partially oxidized Si, just as in the O2 case, which should not occur until the NO (or O<sub>2</sub>) reaches the nearinterfacial region.

# N<sub>2</sub>O oxynitridation

Gas-phase  $N_2O$  decomposition at high temperatures In contrast to NO, which is a relatively stable molecule,  $N_2O$  decomposes rapidly at high temperatures. As we show below, the decomposition is a rather complex process. Gas flow rate, temperature, partial pressure of  $N_2O$  in the oxidizing ambient, reactor type (RTP vs. furnace) and geometry, and impurity levels are parameters which significantly affect the kinetics and the final distribution of products [60, 61, 89, 135].  $N_2O$  also decomposes under UV radiation [136, 137]. The multiparameter nature of the decomposition process makes it difficult to control  $N_2O$  processing and directly compare results obtained from different laboratories. An additional complication is that  $N_2O$  decomposition is an exothermic reaction which may cause nonuniformities of the temperature profile in a reactor [61, 138, 139].

Since NO chemistry has been studied extensively for many years [140] because of its crucial role in combustion reactions and in air pollution, a substantial database of reaction rates and activation energies exists [141]. We used a simple gas-phase reaction model and made computer simulations and analytical studies of the decomposing N2O system, and found it possible to simplify the published mechanisms [79] (for example, Hartig and Tobin [135] use 80 steps) and still obtain similar results, even without including the effects of heat generation and transfer [139] and contaminants (e.g., H<sub>2</sub>O) [135]. What we found is that of the many possible NO reactions known to occur (Table 2), the first five key steps seem to dominate the  $N_2O \rightarrow NO$  decomposition. The rate-limiting one is the first step,  $N_2O \rightarrow N_2 + O$ . The N<sub>2</sub>O decomposition obeys first-order kinetics. The initial rate law for  $N_2O$  decomposition is  $R_0 = 2k_1[N_2O]$ , but rapidly changes to  $R = k_1[N_2O]$  as the reaction proceeds  $(k_1)$  is the reaction constant of the first reaction). The apparent activation energy for the decomposition of N<sub>2</sub>O is 2.5 eV/molecule (2.4  $\times$  10<sup>2</sup> kJ/mol). The characteristic decay time of the N2O concentration is of the order of  $\sim 20$  s at 1000 K (decreasing with temperature). The oxygen atoms then react further by the two key reactions  $N_2O + O \rightarrow 2NO$  and  $N_2O + O \rightarrow N_2 + O_2$ . The branching ratio for these two reactions lies between 0.1 and 0.5 and varies with conditions. The rate law for NO formation is  $R = k_1[N_2O]$ , and the apparent activation energy for the formation of NO is 2.4 eV/molecule  $(2.3 \times 10^2 \text{ kJ/mol}).$ 

As seen from **Figure 11**, the final concentrations of  $N_2$ ,  $O_2$ , and NO obtained using 5-step and 21-step mechanisms over a temperature range of 1000 K-1400 K are as follows:

$$N_2$$
: 65.3%–59.3%,  $O_2$ : 32.0%–25.7%, NO: 2.7%–15.0%; (5 steps)

$$N_2$$
: 65.5%–59.9%,  $O_2$ : 32.2%–26.5%, NO: 2.3%–13.6%. (21 steps)

Data published by Hartig and Tobin [135] (using a much more complex mechanism) report the gas composition of decomposed  $N_2O$  at 1223 K as follows:

N<sub>2</sub>: 62%, O<sub>2</sub>: 28%, NO: 9.5%.

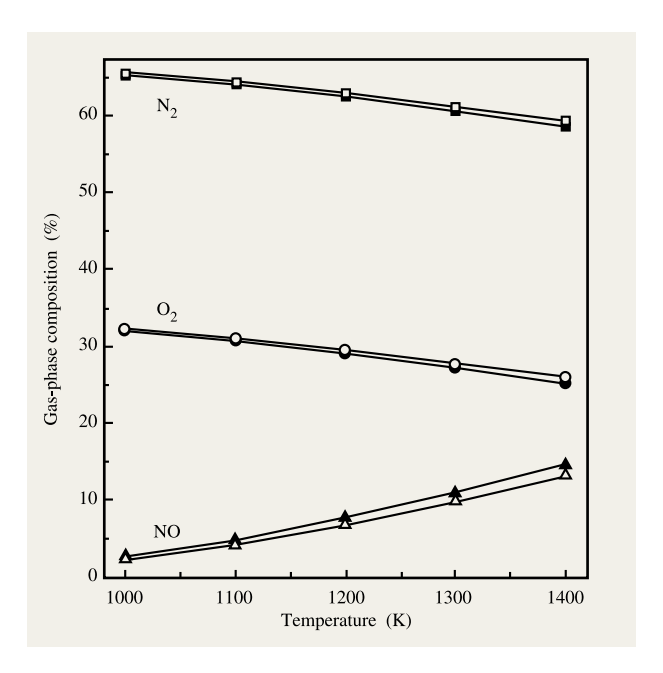
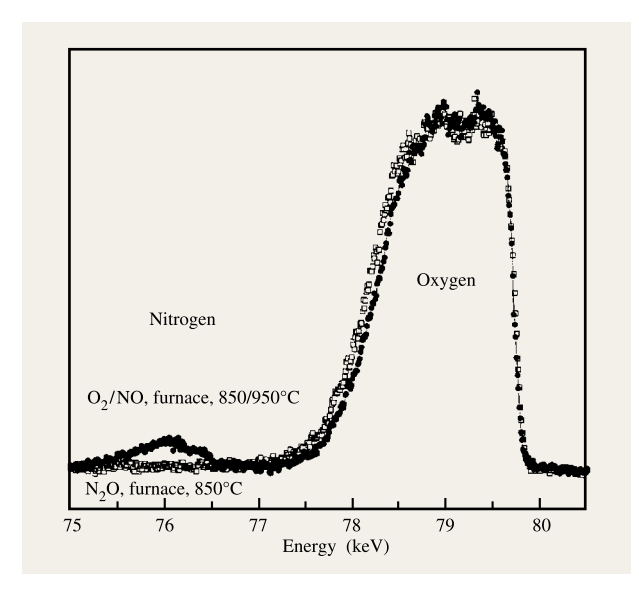


Figure 11

Steady-state composition of the main products  $(N_2, O_2, and NO)$  of gas-phase decomposition of  $N_2O$ , calculated in the scheme discussed in the text (solid symbols – 5 reactions; open symbols – 21 reactions).

This may be compared to  $N_2$ : 64.3%,  $O_2$ : 31.0%, and NO: 4.7% reported by Tobin et al. [89], who extracted the data from the early work of Briner et al. [140]. Finally, we note that the results of the calculations (Figure 11) agree qualitatively with recent mass-spectrometry observations of the gas-phase composition during  $N_2O$  decomposition in a furnace at 1223 K, viz., 61%  $N_2$ , 27%  $O_2$ , and 13% NO [142].

The main products of the N<sub>2</sub>O decomposition are N<sub>2</sub>, O2, NO (with the equilibrium concentration of NO increasing with temperature). Since N<sub>2</sub> is much less reactive than O2 and NO, one could expect that a properly chosen mixture of NO and O, in the gas phase would produce an oxynitride film similar to that grown in N<sub>2</sub>O. However, this is not the case. We observed that oxynitridation in a mixture of NO and O2 (with the variable fraction of NO at 20%, 40%, 60%) is in fact much more similar to NO oxynitridation than to N<sub>2</sub>O oxynitridation [143]. This suggests that there are other active species present during N2O decomposition which are important in the nitridation process. We believe [62], as do others [60, 61], that atomic oxygen plays a key role in N<sub>2</sub>O oxynitridation (see the subsection which follows). Though the equilibrium concentration of O is rather low, an intermediate concentration of atomic oxygen released



MEIS nitrogen and oxygen spectra for the films grown in  $N_2O$  (open symbols) and  $O_2/NO$  (solid symbols). Film thickness is  $\sim 5.5$  nm. The  $O_2/NO$  film has about 1.6 ML (1 ML =  $6.8 \times 10^{14}$  cm<sup>-2</sup>) of nitrogen located within  $\sim 1.5$  nm near the interface. The concentration of N in the  $N_2O$ -grown film is estimated to be less than 0.5 ML but is more broadly distributed in the film (after [74]).

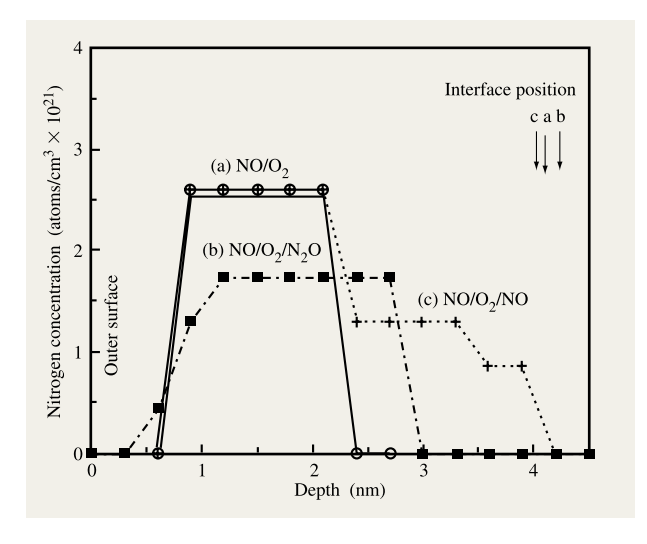


#### Figure 13

MEIS nitrogen depth profiles for an  ${\rm SiO_2}$  film (a) annealed in NO; (b) subsequently annealed at 850°C in  ${\rm N_2O}$ ; or (c) annealed in NO.

in the first step of the decomposition process (Table 2) may be relatively high, especially if N<sub>2</sub>O decomposition

takes place near the wafer. Second, since oxygen radicals are very reactive, even a small partial pressure of atomic oxygen may have a significant effect on oxynitridation. Nitrous oxide ( $N_2O$ ) has even been used in the surface science community to study the interaction of atomic oxygen with Si surfaces [144]. Finally, we note that reactions of  $N_2O$  with the Si wafer and the walls of the reactor may accelerate the decomposition process.

Nitrogen incorporation and removal during N<sub>2</sub>O oxynitridation

Under equivalent conditions, N<sub>2</sub>O yields less nitrogen incorporation than NO. Figure 12 shows MEIS spectra for thin (~5 nm) oxynitride films grown in NO and N<sub>2</sub>O under similar conditions. By integrating the areas under the nitrogen peaks of the spectra, one can readily see that the N<sub>2</sub>O-grown oxynitride has much less incorporated nitrogen. The total concentration of nitrogen increases with temperature (Figure 4) and film thickness [20]. This implies that, in addition to thermal budget considerations, N<sub>2</sub>O processing may not be an efficient source of nitrogen for films thinner than  $\sim$ 3 nm. The nitrogen distribution in the films is sensitive not only to the processing conditions but also to the reactor type [60, 61, 127]. Specifically, SiO<sub>2</sub>N<sub>2</sub> films grown in a furnace and in an RTP reactor have qualitatively different nitrogen depth profiles (Figure 3). The RTN<sub>2</sub>O film shows N pileup near the interface, while the distribution of N in the furnace-grown film is broader. The difference was attributed to the gas-phase chemistry of N<sub>2</sub>O decomposition (see the related subsection) and its subsequent effect on film composition. In the RTN<sub>2</sub>O case, the decomposition takes place near the hot wafer [60, 84], so that most of the decomposition products (including atomic oxygen) can reach the wafer, whereas in a conventional furnace the gas decomposes in the hot inlet of the furnace before it reaches the wafer. This also explains gas-flow effects, i.e., lower nitrogen incorporation rates for lower N<sub>2</sub>O flow rates.

The rate of film growth in  $N_2O$  is much slower than that in  $O_2$  and is related to the amount of nitrogen in the film [20, 32, 142, 145]. Furthermore, the growth rate on the Si(100) surface is slower than that on the (111) and (110) surfaces [146]. Several attempts have been made to model the growth kinetics [82, 88, 142]. A model by Dimitrijev et al. explains the slower growth rate by an exponential (with time) decrease of so-called "reactive sites" near the interface [82]. Other models used a scheme similar to the Deal–Grove model of the thermal oxidation of silicon [88].

The fundamental difference between oxynitridation in  $N_2O$  and NO is that while both incorporate nitrogen (by NO reactions near the interface), in the  $N_2O$  case the nitrogen incorporation occurs simultaneously with nitrogen removal from the upper layers of the film. Saks et al. found in  $N_2O/O_2/N_2O$  studies that the final exposure of

the  $N_2O/O_2$ -grown film (with nitrogen in the middle of the film) to  $N_2O$  results in nitrogen removal from the "bulk" of the film and new nitrogen incorporation near the interface [128]. Similar behavior was also observed in our MEIS studies (**Figure 13**). One can see that for an  $(NO/O_2)$  oxynitride film exposed to  $N_2O$  (i.e.,  $NO/O_2/N_2O$ ), the nitrogen concentration in the middle of the film decreases, whereas for the film annealed in NO (i.e.,  $NO/O_2/NO$ ) this effect was not observed—only incorporation of new nitrogen near the interface takes place. In these studies, the removal was also implied by an acceleration of the film growth.

There have been at least two alternative viewpoints on the mechanism of N removal: Carr et al. [60, 61] proposed that atomic oxygen causes nitrogen removal, whereas Saks et al. [128] argued that NO is responsible. Both NO and O are (intermediate) products of N<sub>2</sub>O gas-phase decomposition at high temperatures (see the related subsection). Our recent NO/O<sub>2</sub>/NO experiments suggest that NO does not effectively remove nitrogen from the oxynitride. On the basis of this observation and the even distribution of nitrogen throughout NO-grown films (except for the topmost layer of the oxide) observed in our work (Figure 8) and by others [37], one can conclude that NO (when directly introduced as a key reactant) has a very low reactivity toward nitrogen removal compared to N<sub>2</sub>O and its decomposition products [60, 128]. Exposure of an oxynitride film to ozone (an effective source of atomic oxygen) causes nitrogen removal from the film, which supports the atomic oxygen hypothesis [60]. However, the role of atomic oxygen in nitrogen removal must be better understood. We note that nitrogen is also removed from the film by a high boron flux from the polysilicon gate [147].

# Mechanisms of nitridation in NO and N<sub>2</sub>O and nitrogen profiles in the film

Figure 14 is a schematic summary of the processes discussed above that occur during silicon (oxy)nitridation.  $N_2O$  rapidly decomposes in the gas phase to  $N_2$  and  $O_3$ and the O then initiates a further series of reactions to form NO, the key oxynitriding agent, and other species. NO is similar to O, when it interacts with Si and SiO, in that the dominant oxynitride growth mechanism involves NO diffusion through an SiO<sub>x</sub>N<sub>y</sub> overlayer, followed by a reaction with silicon at and near the SiO<sub>2</sub>N<sub>2</sub>/Si interface. The thermochemistry of the system is such that nitrogen, although thermodynamically unstable in the growing film relative to oxygen, appears to become kinetically trapped at the SiO<sub>2</sub>/Si interface during growth. Alternatively, it may lower the interfacial stress, and therefore be stable only near the interface. The final nitrogen concentration and distribution is influenced by a competition between N incorporation and removal. The removal reaction is likely

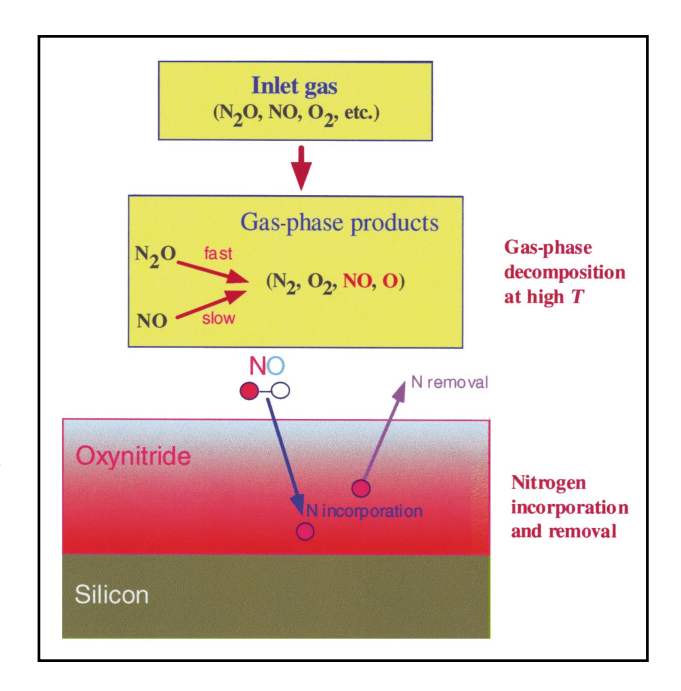


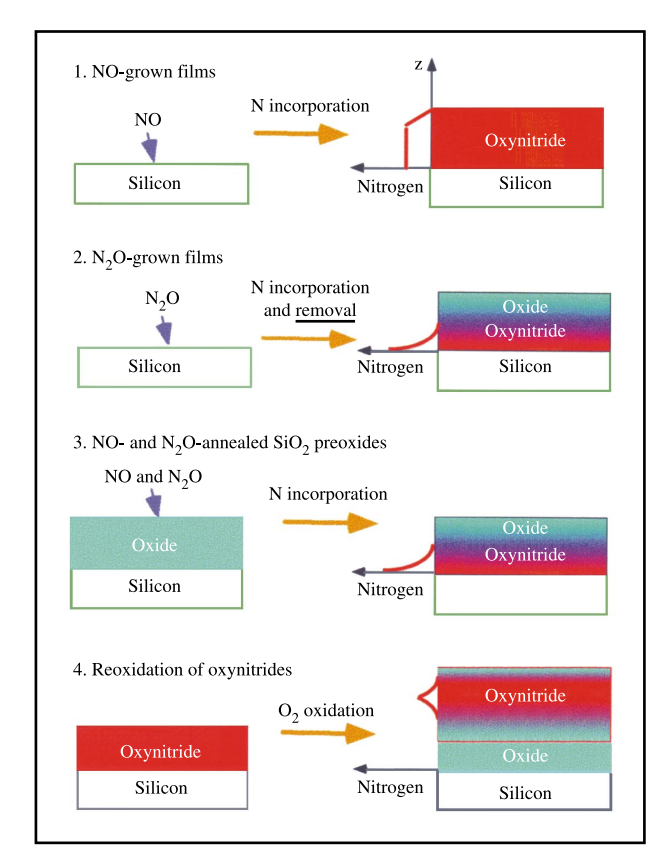
Figure 14 Schematic model of silicon oxynitridation in NO or  $N_2O$ .

due to atomic oxygen. Since the reactivities of NO,  $N_2O$ , and  $O_2$  with Si,  $SiO_2$ , and  $SiO_xN_y$  are quite different, properly chosen sequences of thermal reactions with Si can lead to oxynitride films with different nitrogen concentrations and profiles, and therefore electrical properties.

As an illustration, in **Figure 15** we schematically present several reaction sequences and resultant N profiles that we (and others) have observed. We note that most of the reactions are very condition-dependent; as pressure, film thickness, heating mode (conventional furnace vs. rapid thermal), etc. are changed, the N profiles can change significantly.

#### • *Nitridation in N*,

Though molecular nitrogen is believed to be relatively inert, it was observed in early papers that annealing of  $SiO_2$  films in  $N_2$  results in the initial reduction of fixed oxide charge [98]. This behavior was attributed to the formation of an  $SiO_xN_y$  layer near the interface as monitored by XPS [87]. These nitridation reactions were performed in a furnace at high temperature (>925°C) for  $\ge 1$  hr (i.e., requiring a high thermal budget). To reduce the thermal budget, we grew oxynitrides in nominally pure  $N_2$  by rapid thermal processing [80]. We use the term "nominally" to mean that although the input  $N_2$  gas stream is purified at the point of use and therefore extremely free of contaminants (less than 1 ppb each



Nitrogen depth distributions for different nitridation sequences.

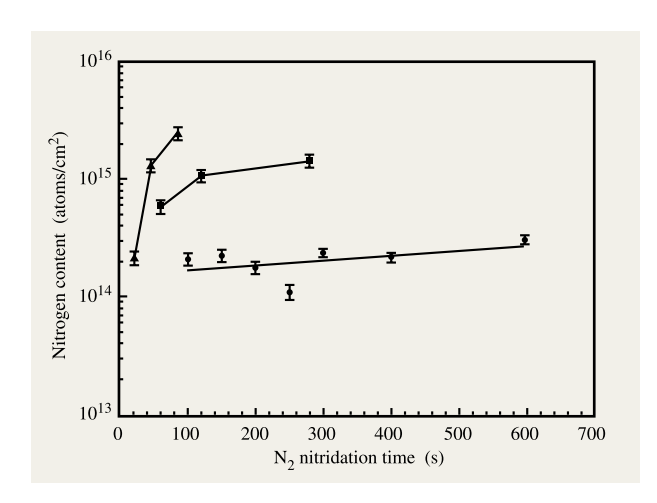


#### Figure 16

Kinetics of nitrogen accumulation during RTN<sub>2</sub> processing at 850°C (circles), 950°C (squares), and 1050°C (triangles) (after [80]).

of  $\rm H_2O$ ,  $\rm O_2$ ,  $\rm CO_2$ , and  $\rm CO$ ), a cold-wall RTP module contributes impurities to the ambient through outgassing from the walls. Although the  $\rm Si/N_2$  system may be relatively inert for  $T < 1200^{\circ}\rm C$ , the  $\rm Si/N_2/H_2O/H_2/O_2$  system is probably not. Thus, we observed that  $\rm N_2$  reacts with Si at moderate temperatures (850–1050°C) in an RTP module (due to the presence of gas-phase impurities) to form ultrathin (less than 1.2 nm) films as measured by ellipsometry (using n = 1.47), cross-sectional TEM, and MEIS.

Figure 16 illustrates nitrogen content (measured by NRA) as a function of N<sub>2</sub> nitridation time for RTN<sub>2</sub> treatment at various temperatures [80]. At 850°C, the nitrogen content is almost constant with time, whereas at the higher temperatures it increases and then may saturate with time. It can be seen from Figure 16 that anywhere from 0.2 to 3 ML of nitrogen can be incorporated, depending upon temperature and time. Figure 17 is a plot of the ratio N/(N + O) as a function of RTN, time at 850, 950, and 1050°C. The ratio increases with increasing temperature and time, and appears to approach that of the high-temperature stoichiometric compound Si<sub>2</sub>N<sub>2</sub>O. The RTN<sub>2</sub> films may consist of amorphous mixtures of SiO<sub>2</sub> and Si<sub>2</sub>N<sub>2</sub>O. Mixtures of Si<sub>2</sub>N<sub>2</sub>O, Si<sub>3</sub>N<sub>4</sub>, and SiO<sub>2</sub> phases have similarly been observed in plasmadeposited oxynitrides [148]. Oxygen and nitrogen depth profiling by MEIS shows a fairly uniform distribution of the elements in the films.

#### • Nitridation in NH,

Nitridation in ammonia was one of the first methods used to incorporate relatively high ( $\sim 10-15$  at.%) concentrations of nitrogen into SiO<sub>2</sub> films [3, 10, 11, 59, 96]. XPS and AES depth profiles show that nitrogen piles up both at the interface and at the outer surface during the initial stages of nitridation [149]. The nitrogencontaining region near the interface was reported to be about 3 nm wide. As nitridation time increases, the concentration of nitrogen slowly increases, and the distribution becomes more uniform throughout the film [10, 11]. The thickness of the film remains essentially unchanged during nitridation. Nitrogen incorporation is enhanced by decreasing the SiO<sub>2</sub> film thickness [10, 11].

The nitridation atmosphere of  $\mathrm{NH_3}$  introduces high concentrations of hydrogen into  $\mathrm{SiO_2}$  films, which then can act as traps. SIMS analysis shows that the hydrogen concentration increases monotonically with nitridation time and becomes higher for higher temperatures. The hydrogen tends to pile up near the interface [150]. It has been shown that the high concentration of hydrogen can be reduced by a postnitridation anneal in a hydrogen-free ambient (e.g.,  $\mathrm{N_2}$ ). It has also been found that the rate of hydrogen reduction is not dependent on the annealing gas ( $\mathrm{N_2}$  or  $\mathrm{O_2}$ ), indicating thermally activated out-diffusion

of hydrogen from the film [10, 11]. Because of the detrimental effects of hydrogen on device performance, lighter nitridation (lower temperature, shorter time) is desirable, since it introduces less hydrogen into the film.

Finally, we note that ammonia can be used for direct nitridation of Si. In this reaction scheme, NH<sub>3</sub> reacts with the Si surface at high temperatures to produce an ultrathin layer of silicon nitride [151–153], although again caution must be taken to minimize oxygen incorporation if it is not desired.

# 6. Nitridation by chemical and physical deposition methods

In this section, we briefly outline some deposition techniques for preparing ultrathin (oxy)nitride films. More details about deposition techniques can be found in review papers [19, 40]. CVD methods, using the existing "infrastructure" of commercially available reactors and precursors, are employed in many different silicon processing steps. High-temperature (~800°C) deposition of oxynitrides can be performed by reacting SiH<sub>4</sub> (or SiH<sub>2</sub>Cl<sub>2</sub>) with a mixture of N<sub>2</sub>O and NH<sub>3</sub>. Without ammonia in the gas phase, no nitrogen incorporation takes place; only SiO<sub>2</sub> is deposited. The composition of the film, stress, refractive index, and growth rate are dependent on the flow rate. The concentration of incorporated nitrogen (and hydrogen) increases with an increase in the ratio of NH<sub>3</sub>/N<sub>2</sub>O flow rate. The viability of this technique has been demonstrated for making device-quality ultrathin (~3-4 nm) nitrided SiO, films and oxide/nitride stacks [18]. For this, reduced pressures of the reactants and RTP reactors are used. As with most other deposition methods, CVD requires postdeposition treatment to stabilize the film structure, drive hydrogen out, and minimize electrical defects. Figure 18 shows nitrogen MEIS depth profiles for a 4-nm-thick RTCVD-deposited film (800°C, 3 Torr, N<sub>2</sub>O flow rate of 500 sccm, NH<sub>2</sub>/N<sub>2</sub>O ratio of 0.05, and SiH<sub>4</sub>/N<sub>2</sub>O ratio of 0.0128) after annealing in Ar, O<sub>2</sub>, and N<sub>2</sub>O. One can see that the film annealed in Ar has nitrogen distributed almost evenly in the film, while annealing in N<sub>2</sub>O causes nitrogen removal from the film, as discussed in the subsection on nitrogen incorporation and removal during N2O oxynitridation. Finally, we note the interesting idea of oxynitride deposition at quite low temperature (330°C) using photo-enhanced CVD of Si<sub>2</sub>H<sub>6</sub>, NH<sub>2</sub>, and NO<sub>3</sub> [154].

Plasma-assisted nitridation is a well-known deposition method for low-temperature processing [19, 40, 49, 155]. First discussed in the 1970s, several reaction schemes and different reactor types (e.g., rf, ECR, etc.) have been reported for plasma-enhanced deposition of silicon nitride. The traditional scheme includes the reaction of  $\rm SiH_4$  and  $\rm NH_3$  in a plasma at 200–400°C. The use of  $\rm N_2$  instead of ammonia helps to reduce the hydrogen content in the film;

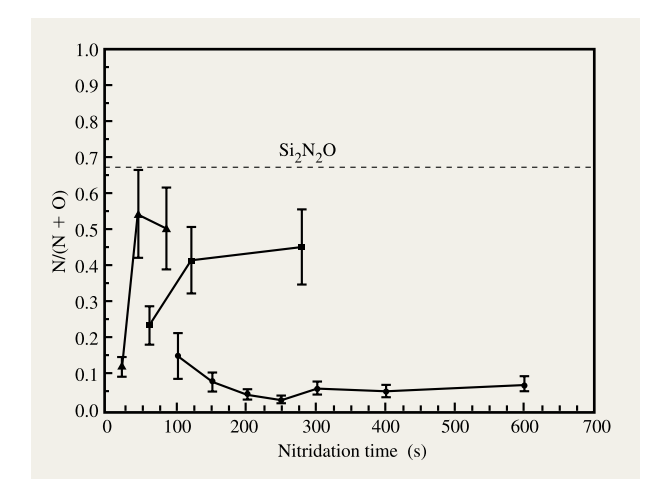


# Figure 17

Ratio of N/(N + O) in ultrathin films grown by RTN $_2$  processing at 850°C (circles), 950°C (squares), and 1050°C (triangles). The dashed line shows the ratio for the Si $_2$ N $_2$ O oxynitride phase (after [29, 80]).

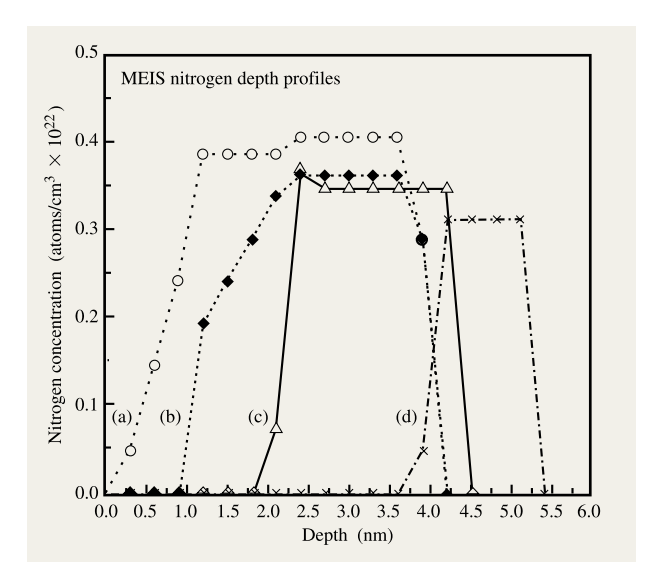
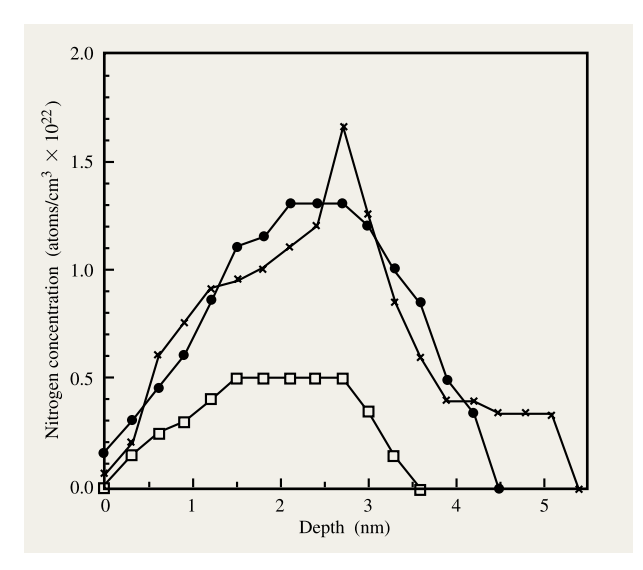


# Figure 18

MEIS nitrogen depth profiles for an oxynitride film grown by an RTCVD method annealed in (a) Ar at 800°C for 30 s; (b)  $O_2$  at 1000°C for 30 s; (c)  $N_2O$  at 900°C for 15 s; and (d)  $N_2O$  at 1000°C for 30 s. The samples were made by E. Vogel and J. J. Wortman (NCSU).

however, ionization of nitrogen is more difficult.  $N_2O$  can also be used for plasma-assisted nitridation of ultrathin SiO<sub>2</sub> films. To minimize the damage to the substrate by



MEIS nitrogen depth profiles for an  $\sim$ 3.5-nm SiO<sub>2</sub> film implanted with nitrogen ions with an energy of 200 eV (squares), 500 eV (solid circles), and 1000 eV (crosses). The implantation dose is  $10^{16}$  ions/cm<sup>2</sup>.

energetic particles, a remote plasma deposition method has been developed [19]. In this process, the nitrogen-containing species are plasma-excited outside the reactor chamber. Then the excited species are extracted from the plasma region and react with the substrate. As in the case of the conventional CVD process, the composition of the film is determined in part by the ratio of gas flow of the reactive species. More details about plasma-assisted nitridation can be found in review papers [19].

Another nitridation technique based on energetic nitrogen particles is low-energy ion implantation [45–47, 50-52, 55, 84, 156]. The nitridation of the gate-oxide film can be performed in two different sequences: low-energy nitrogen ions can be implanted into already grown oxide, or nitrogen can be implanted into the silicon substrate, which is subsequently oxidized [83, 84, 156]. In the former case, the energy of the nitrogen ions should be low enough to avoid penetration (and damage) to the silicon substrate. The penetration depth of the ions decreases with ion energy. As a reference, the penetration depth of 1-keV nitrogen ions in SiO, is about 4 nm and decreases to  $\sim 2.3$  nm for 0.5-keV ions, which sets a limit for the ion energies for ultrathin oxides. Figure 19 shows MEIS nitrogen depth distributions for an ~3.5-nm SiO, film nitrided by implantation of nitrogen ions of different energies. These data illustrate the increasing penetration depth and concentration of incorporated nitrogen (for the same dose) with ion energy. The mechanism of low-energy implantation is different from that of conventional highenergy implantation [55]. When the low-energy ion approaches the surface, it becomes neutralized within about 1 nm of the surface. As a result, the nitridation is then caused by diffusion, reaction, and desorption of this hot nitrogen atom. Owing to desorption (and sputtering) steps, this complex process typically results in a concentration of implanted nitrogen that is lower than the implantation dose. When the nitrogen ions are implanted into the silicon prior to the oxidation, a reduction in reliability is observed [156]. Subsequent high-temperature oxidation results in the loss of some nitrogen, and its segregation and accumulation near the interface, which in turn leads to improved electrical properties.

The recently developed jet vapor deposition (JVD) method utilizes a high-speed jet of a light carrier gas to transport the relevant species onto the Si substrate to form nitride films at room temperature [43]. In this process, diluted silane and a mixture of N<sub>2</sub> + He flow through nozzles into a microwave discharge region near the outer nozzle exit. Reactive Si species and N atoms formed in the discharge region are transported in the sonic He jet to the Si substrate, where they form a nitride. The film composition and growth rate are determined by the SiH<sub>4</sub>/He/N<sub>2</sub> ratio and the flow rate. This technique has been shown to be capable of producing device-quality (both capacitors and transistors) ultrathin films. However, the uniformity of ultrathin films deposited over a large wafer (limited by the small size of the nozzle) and oxygen incorporated into the film are of concern for practical applications.

Atomic layer deposition, or ALD (also known as atomic layer epitaxy, ALE, or atomic layer CVD, AL-CVD), a technique based on selective reactivity of gaseous and surface species, allows one to produce in a controlled matter ultrathin films with a rate of approximately one monolayer per deposition cycle [157, 158]. This technique has been used to deposit thin films of various dielectric materials, including SiO2. However, to the best of our knowledge, a procedure for preparing nitrided SiO, films by ALD has not yet been established. Goto et al. proposed a process of making thin (2-10 nm) silicon nitride films by repetitive plasma nitridation cycles of Si by NH<sub>2</sub> and deposition of Si by SiH<sub>2</sub>Cl<sub>2</sub> thermal reaction [44]. The deposition rate was found to be nearly half a monolayer per deposition cycle, and the deposited films showed thickness uniformity much better than that of remote plasma CVD films [44].

Finally, we note that very reactive nitrogen atoms can be used for Si and  $SiO_2$  nitridation, as was demonstrated in early studies [53, 54]. The interaction of nitrogen atoms with a silicon surface can produce a thin ( $\sim$ 2–3 nm) layer of silicon nitride. However, the practical use of the nitrogen atoms in the near future may be limited by

the lack of available sources of atomic nitrogen that can generate a uniform beam over a large wafer.

# 7. Nitrogen engineering of ultrathin nitrided oxides

On the basis of our understanding of the kinetics and thermodynamics of nitrogen incorporation in  $\mathrm{SiO}_2$ , ultrathin oxynitride films with nitrogen-enhanced layers located in specific regions of a film can be achieved. Both thermal nitridation methods and deposition techniques can be used. To tailor the nitrogen content and distribution within the ultrathin dielectric by a thermal method, one can employ the fact that  $\mathrm{N}_2\mathrm{O}$ ,  $\mathrm{NO}$ , and  $\mathrm{O}_2$  gases behave differently with respect to nitrogen incorporation and removal, as discussed in the subsection on nitrogen incorporation and removal during  $\mathrm{N}_2\mathrm{O}$  oxynitridation.

One thermal process scheme that we have used to achieve a double-peaked nitrogen profile is as follows [81]. First, a thin oxide layer containing a high concentration of nitrogen is grown by reacting NO with Si. (Other surface nitridation methods may also work, though some of the techniques, for example N<sub>2</sub>O oxynitridation, may yield an insufficient concentration of nitrogen in ultrathin films [33].) The oxynitride film is then reoxidized in O<sub>2</sub>, which results in a new oxide layer grown beneath the original oxynitride. We and others have demonstrated that such reoxidation does not significantly change the already incorporated nitrogen concentration [62, 128]. In the third step, the sample is nitrided in NO—a key step. NO diffuses to the interface and does not remove nitrogen from the interior of the film [62, 76]. Therefore, the top nitrogen peak remains undisturbed. The MEIS results (Figure 20) clearly demonstrate that the NO/O<sub>2</sub>/NO sample has nitrogen-enhanced layers located near both the top (SiO<sub>2</sub>/polysilicon) and bottom (Si/SiO<sub>2</sub>) of the oxynitride film. One can see that a longer third-step NO annealing time (40 min) results in a higher concentration of nitrogen near the interface. In this scheme, one should be careful using N<sub>2</sub>O in the final step, because it removes incorporated nitrogen. Finally, we note that nitrogenlayered structures can also be produced by deposition methods [18, 19, 41, 49]) or by a combination of thermal nitridation/deposition methods.

# Acknowledgments

The authors wish to thank L. C. Feldman, G. Lucovsky, D. Buchanan, H. Du, and M. Copel for useful discussions; D. Brasen and T. Sorsch for their help with oxynitride films by thermal methods; W. Lennard, I. Baumvol, and F. Stedile for nuclear reaction analysis; and E. Vogel and J. J. Wortman, who collaborated with us on LPCVD oxynitrides. The Rutgers group acknowledges support from NSF under Grant No. DMR-9705367 and from SRC under Grant No. 97-BJ-451.

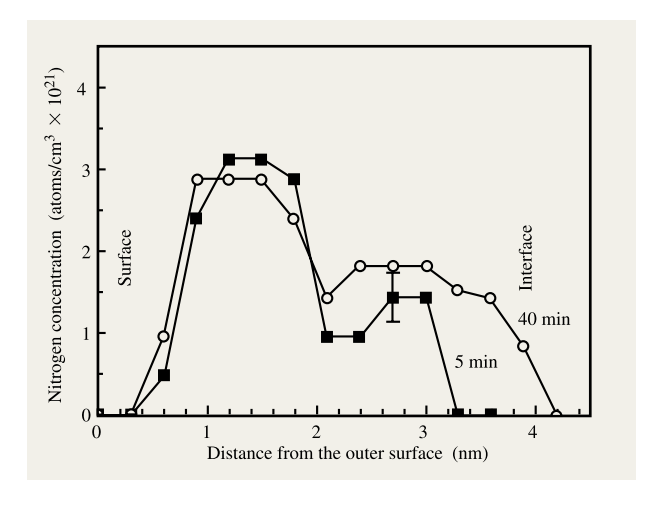


#### Figure 20

Nitrogen double-layered structure produced by an NO/O<sub>2</sub>/NO processing for two different times of the final NO anneal: 5 min (squares) and 40 min (circles) (after [81]).

#### References

- The National Technology Roadmap for Semiconductors, Semiconductor Industry Association, San Jose, CA, 1997.
- P. Balk, "Dielectrics for Field Effect Technology," Adv. Mater. 7, 703 (1995).
- T. Hori, Gate Dielectrics and MOS ULSI, Springer, Berlin, 1997.
- L. Feldman, E. P. Gusev, and E. Garfunkel, "Ultrathin Dielectrics in Si Microelectronics—An Overview," Fundamental Aspects of Ultrathin Dielectrics on Si-based Devices, E. Garfunkel, E. P. Gusev, and A. Y. Vul', Eds., Kluwer Academic Publishers, Dordrecht, Netherlands, 1998, p. 1.
- 5. M. T. Bohr, "Technology Development Strategies for the 21st Century," *Appl. Surf. Sci.* **100/101**, 534 (1996).
- Y. Taur, D. Buchanan, W. Chen, D. J. Frank, K. I. Ismail, S.-H. Lo, G. A. Sai-Halasz, R. G. Viswanathan, H.-J. C. Wann, S. J. Wind, and H.-S. Wong, "CMOS Scaling into the Nanometer Regime," *Proc. IEEE* 85, 486 (1997).
- D. A. Buchanan and S. H. Lo, "Reliability and Integration of Ultrathin Gate Dielectrics for Advanced CMOS," *Microelectron. Eng.* 36, 13 (1997).
- 8. H. Hwang, W. Ting, B. Maiti, D. L. Kwong, and J. Lee, "Electrical Characteristics of Ultrathin Oxynitride Gate Dielectrics Prepared by Rapid Thermal Oxidation of Silicon in N<sub>2</sub>O," *Appl. Phys. Lett.* **57**, 1010 (1990).
- H. Fukuda, T. Arakawa, and S. Ohno, "Highly Reliable Thin Nitrided SiO<sub>2</sub> Films Formed by Rapid Thermal Processing in an N<sub>2</sub>O Ambient," *Jpn. J. Appl. Phys.* 29, L2333 (1990).
- T. Hori, S. Ákamatsu, and Y. Odake, "Deep-Submicrometer Technology with Reoxidized or Annealed Nitrided-Oxide Gate Dielectrics Prepared by Rapid Thermal Processing," *IEEE Trans. Electron Devices* 39, 118 (1992).
- 11. T. Hori, "Nitrided Gate Oxide CMOS Technology for Improved Hot-Carrier Reliability," *Microelectron. Eng.* **22**, 245 (1993).

- 12. E. C. Carr and R. A. Buhrman, "Role of Interfacial Nitrogen in Improving Thin Silicon Oxides Grown in N<sub>2</sub>O," *Appl. Phys. Lett.* **63**, 54 (1993).
- H. T. Tang, W. N. Lennard, M. Zinke-Allmang, I. V. Mitchell, L. C. Feldman, M. L. Green, and D. Brasen, "Nitrogen Content of Oxynitride Films on Si(100)," *Appl. Phys. Lett.* 64, 64 (1994).
- M. Bhat, L. K. Han, D. Wristers, J. Yan, D. L. Kwong, and J. Fulford, "Effect of Chemical Composition on the Electrical Properties of NO-Nitrided SiO<sub>2</sub>," *Appl. Phys. Lett.* 66, 1225 (1995).
- D. Landheer, Y. Tao, D. X. Xu, G. I. Sproule, and D. A. Buchanan, "Defects Generated by Fowler-Nordheim Injection in Silicon Dioxide Films Produced by Plasma-Enhanced Chemical-Vapour Deposition with Nitrous Oxide and Silane," J. Appl. Phys. 78, 1818 (1995).
- S. V. Hattangady, H. Niimi, and G. Lucovsky, "Controlled Nitrogen Incorporation at the Gate Oxide Surface," Appl. Phys. Lett. 66, 3495 (1995).
- D. M. Fleetwood and N. M. Saks, "Oxide, Interface, and Border Traps in Thermal, N<sub>2</sub>O, and N<sub>2</sub>O Nitrided Oxides," J. Appl. Phys. 79, 1583 (1996).
- W. L. Hill, E. M. Vogel, V. Misra, P. K. McLarty, and J. J. Wortman, "Low Pressure Rapid Thermal CVD of Oxynitride Gate Dielectrics for N-Channel and P-Channel MOSFET's," *IEEE Trans. Electron Devices* 43, 15 (1996).
- G. Lucovsky, "Spatially-Selective Incorporation of Bonded-Nitrogen into Ultrathin Gate Dielectrics by Low-Temperature Plasma-Assisted Processing," Fundamental Aspects of Ultrathin Dielectrics on Si-based Devices, E. Garfunkel, E. P. Gusev, and A. Y. Vul', Eds., Kluwer Academic Publishers, Dordrecht, Netherlands, 1998, p. 147.
- M. L. Green, "Rapid Thermal O<sub>2</sub>-Oxidation and N<sub>2</sub>O-Oxynitridation," Advances in Rapid Thermal and Integrated Processing, F. Roozeboom, Ed., Kluwer Academic Publishers, Dordrecht, Netherlands, 1995, p. 193.
- H. B. Harrison, H. F. Li, S. Dimitrijev, and P. Tanner, "Nitrogen in Ultrathin Dielectrics," Fundamental Aspects of Ultrathin Dielectrics on Si-based Devices, E. Garfunkel, E. P. Gusev, and A. Y. Vul', Eds., Kluwer Academic Publishers, Dordrecht, Netherlands, 1998, p. 191.
- M. Alessandri, C. Clementi, B. Crivelli, G. Ghidini,
   F. Pellizzer, F. Martin, M. Imai, and H. Ikegawa,
   "Nitridation Impact on Thin Oxide Charge Trapping,"
   Microelectron. Eng. 36, 211 (1997).
- T. Matsuoka, S. Taguchi, K. Taniguchi, C. Hamaguchi, S. Kakimoto, and J. Takagi, "Thickness Dependence of Furnace N<sub>2</sub>O-Oxynitridation Effects on Breakdown of Thermal Oxides," *IEICE Trans. Electron.* E78-C, 248 (1995).
- T. Matsuoka, S. Taguchi, H. Ohtsuka, K. Taniguchi, C. Hamaguchi, S. Kakimoto, and K. Uda, "Hot-Carrier-Induced Degradation of N<sub>2</sub>O-Oxynitrided Gate Oxide NMOSFETs," *IEEE Trans. Electron Devices* 43, 1364 (1996).
- E. Cartier, D. A. Buchanan, and G. J. Dunn, "Atomic Hydrogen-Induced Interface Degradation of Reoxidized-Nitrided Silicon Dioxide on Silicon," *Appl. Phys. Lett.* 64, 901 (1994).
- D. M. Brown, P. V. Gray, F. K. Heumann, H. R. Philipp, and E. A. Taft, "Properties of Si<sub>x</sub>O<sub>y</sub>N<sub>z</sub> Films on Si," J. Electrochem. Soc. 115, 311 (1968).
- V. A. Gritsenko, Structure and Electronic Properties of Amorphous Insulators in Silicon MIS Structures, Science, Novosibirsk, Russia, 1993.
- D. Wristers, L. K. Han, T. Chen, H. H. Wang, and D. L. Kwong, "Degradation of Oxynitride Gate Dielectric

- Reliability Due to Boron Diffusion," Appl. Phys. Lett. 68, 2094 (1996).
- 29. M. L. Green, D. Brasen, L. Feldman, E. Garfunkel, E. P. Gusev, T. Gustafsson, W. N. Lennard, H. C. Lu, and T. Sorsch, "Thermal Routes to Ultrathin Oxynitrides," Fundamental Aspects of Ultrathin Dielectrics on Si-based Devices, E. Garfunkel, E. P. Gusev, and A. Y. Vul', Eds., Kluwer Academic Publishers, Dordrecht, Netherlands, 1998, p. 181.
- D. Bouvet, P. A. Clivaz, M. Dutoit, C. Coluzza,
   J. Almeida, G. Margaritondo, and F. Pio, "Influence of Nitrogen Profile on Electrical Characteristics of Furnaceor Rapid Thermally Nitrided Silicon Dioxide Films,"
   J. Appl. Phys. 79, 7114 (1996).
- Z. Q. Yao, H. B. Harrison, S. Dimitrijev, and Y. T. Yeow, "Effects of Nitric Oxide Annealing of Thermally Grown Silicon Dioxide Characteristic," *IEEE Electron Device Lett.* 16, 345 (1995).
- M. L. Green, D. Brasen, L. C. Feldman, W. Lennard, and H. T. Tang, "Effect of Incorporated Nitrogen on the Kinetics of Thin Rapid Thermal N<sub>2</sub>O Oxides," *Appl. Phys. Lett.* 67, 1600 (1995).
- 33. M. L. Green, D. Brasen, K. W. Evans-Lutterodt, L. C. Feldman, K. Krisch, W. Lennard, H. T. Tang, L. Manchanda, and M. T. Tang, "RTO of Silicon in N<sub>2</sub>O Between 800 and 1200°C: Incorporated Nitrogen and Roughness," *Appl. Phys. Lett.* 65, 848 (1994).
- 34. R. I. Hedge, P. J. Tobin, K. G. Reid, B. Maiti, and S. A. Ajuria, "Growth and Surface Chemistry of Oxynitride Gate Dielectric Using Nitric Oxide," *Appl. Phys. Lett.* 66, 2882 (1995).
- Z. H. Lu, S. P. Tay, R. Cao, and P. Pianetta, "The Effect of Rapid Thermal N<sub>2</sub>O Oxynitridation on the Oxide/Si(100) Interface Structure," *Appl. Phys. Lett.* 67, 2836 (1995).
- D. G. J. Sutherland, H. Akatsu, M. Copel, F. J. Himpsel, T. Callcott, J. A. Carlisle, D. Ederer, J. J. Jia, I. Jimenez, R. Perera, D. K. Shuh, L. J. Terminello, and W. M. Tong, "Stoichiometry Reversal in the Growth of Thin Oxynitride Films on Si(100) Surfaces," J. Appl. Phys. 78, 6761 (1995).
- 37. Z. Q. Yao, "The Nature and Distribution of Nitrogen in Silicon Oxynitride Grown on Si in a Nitric Oxide Ambient," *J. Appl. Phys.* **78**, 2906 (1995).
- 38. J. J. Ganem, S. Rigo, I. Trimaille, I. J. R. Baumvol, and F. C. Stedile, "Dry Oxidation Mechanisms of Thin Dielectric Films Formed Under N<sub>2</sub>O Using Isotopic Tracing Methods," *Appl. Phys. Lett.* 68, 2366 (1996).
- M. Copel, R. M. Tromp, H. J. Timme, K. Penner, and T. Nakao, "Effects of Surface Oxide on Rapid Thermal Nitridation of Si(100)," J. Vac. Sci. Technol. A 14, 462 (1996).
- F. H. P. M. Habraken and A. E. T. Kuiper, "Silicon Nitride and Oxynitride Films," *Mater. Sci. Eng. Rep.* R12, 123 (1994).
- S. V. Hattangady, H. Niimi, and G. Lucovsky, "Integrated Processing of Silicon Oxynitride Films by Combined Plasma and Rapid-Thermal Processing," *J. Vac. Sci. Technol. A* 14, 3017 (1996).
- 42. E. P. Gusev, H. C. Lu, T. Gustafsson, E. Garfunkel, M. L. Green, and D. Brasen, "The Composition of Ultrathin Oxynitrides Thermally Grown in NO," *J. Appl. Phys.* **82**, 896 (1997).
- 43. T. P. Ma, "Gate Dielectric Properties of Silicon Nitride Films Formed by Jet Vapor Deposition," *Appl. Surf. Sci.* **117/118**, 259 (1997).
- 44. H. Goto, K. Shibahara, and S. Yokoyama, "Atomic Layer Controlled Deposition of Silicon Nitride with Self-Limiting Mechanism," *Appl. Phys. Lett.* 68, 3257 (1996).
- 45. W. DeCoster, B. Brijs, H. Bender, J. Alay, and W. Vandervorst, "RBS, AES, and XPS Analysis of Ion Beam

- Induced Nitridation of Si and SiGe Alloys," *Vacuum* **45**, 389 (1994).
- 46. O. C. Hellman, N. Herbots, and O. Vancauwenberghe, "Kinetics of Ion Beam Nitridation (IBM) of Si and MBE-Grown Ge and Si Ge<sub>1-x</sub> Alloys: The Role of Ion Energy, Ion Dose and Substrate Temperature," *Nucl. Instr. Meth. B* 67, 301 (1992).
- 47. R. Hezel and N. Lieske, "Room Temperature Formation of Si-Nitride Films by Low Energy Ion Implantation into Silicon," *J. Electrochem. Soc.* **129**, 379 (1982).
- H. Kobayashi, T. Mizokuro, Y. Nakato, K. Yoneda, and Y. Todokoro, "Nitridation of Silicon Oxide Layers by Nitrogen Plasma Generated by Low Energy Electron Impact," Appl. Phys. Lett. 71, 1978 (1997).
- R. Kraft, T. P. Schneider, W. W. Dostalik, and S. Hattangady, "Surface Nitridation of Silicon Dioxide with a High Density Nitrogen Plasma," J. Vac. Sci. Technol. B 15, 967 (1997).
- 50. J. S. Pan, A. T. S. Wee, C. H. A. Huan, H. S. Tan, and K. L. Tan, "AES Analysis of Nitridation of Si(100) by 2–10 keV N<sub>2</sub><sup>+</sup> Ion Beams," *Appl. Surf. Sci.* 115, 166 (1997).
- K. H. Park, B. C. Kim, and H. Kang, "Kinetic Energy Dependence of N<sup>+</sup> and N<sub>2</sub><sup>+</sup> Reactions with Si(100)," Surf. Sci. 283, 73 (1993).
- 52. Z.-M. Ren, Z.-F. Ying, X.-X. Xiong, M.-Q. He, F.-M. Li, Y.-C. Du, and L.-Y. Cheng, "Study of the Growth of Thin Nitride Films Under Low-Energy Nitrogen-Ion Bombardment," Appl. Phys. A 58, 395 (1994).
- 53. A. G. Schrott and S. C. Fain, "Nitridation of Si(111) by Nitrogen Atoms," Surf. Sci. 111, 39 (1981).
- A. G. Schrott, Q. X. Su, and S. C. Fain, "Reaction of Si(100) Single Crystals with Nitrogen Atoms," Surf. Sci. 123, 223 (1982).
- J. A. Taylor, G. M. Lancaster, A. Ignatiev, and J. W. Rabalais, "Interaction of Ion Beams with Surfaces. Reaction of Nitrogen with Silicon and Its Oxides," J. Chem. Phys. 68, 1776 (1978).
- G. Lucovsky, A. Banerjee, B. Hinds, B. Claffin, K. Koh, and H. Yang, "Minimization of Sub-Oxide Transition Regions at Si-SiO<sub>2</sub> Interfaces by 900°C Rapid Thermal Annealing," *Microelectron. Eng.* 36, 207 (1997).
- M. Hillert, S. Jonsson, and B. Sundman, "Thermodynamic Calculation of the Si-N-O System," Z. Metallkd. 83, 648 (1992).
- H. Du, R. E. Tressler, and K. E. Spear, "Thermodynamics of the Si-N-O System and Kinetic Modelling of Oxidation of Si<sub>3</sub>N<sub>4</sub>," *J. Electrochem. Soc.* 136, 3210 (1989).
- 59. I. J. R. Baumvol, F. C. Stedile, J. J. Ganem, I. Trimaille, and S. Rigo, "Isotopic Tracing During Rapid Thermal Growth of Silicon Oxynitride Films on Si in O<sub>2</sub>, NH<sub>3</sub>, and N<sub>2</sub>O," *Appl. Phys. Lett.* 70, 2007 (1997).
- E. C. Carr, K. A. Ellis, and R. A. Buhrman, "Nitrogen Profiles in Thin SiO<sub>2</sub> in N<sub>2</sub>O: The Role of Atomic Oxygen," *Appl. Phys. Lett.* 66, 1492 (1995).
- K. A. Ellis and R. A. Buhrman, "Furnace Gas-Phase Chemistry of Silicon Oxynitridation in N<sub>2</sub>O," *Appl. Phys. Lett.* 68, 1696 (1996).
- H. C. Lu, E. P. Gusev, T. Gustafsson, M. L. Green,
   D. Brasen, and E. Garfunkel, "Compositional and Mechanistic Aspects of Ultrathin Oxynitride Film Growth on Si(100)," *Microelectron. Eng.* 36, 29 (1997).
- 63. H. C. Lu, E. P. Gusev, T. Gustafsson, and E. Garfunkel, "The Effect of Near-Interfacial Nitrogen on the Oxidation Behavior of Ultrathin Silicon Oxynitrides," *J. Appl. Phys.* 81, 6992 (1997).
- 64. C. R. Helms and E. H. Poindexter, "The Si–SiO<sub>2</sub> System: Its Microstructure and Imperfections," *Rep. Prog. Phys.* **57**, 791 (1994).
- 65. E. Irene, "Models for the Oxidation of Silicon," CRC

- Crit. Rev. Solid State Mater. Sci. 14, 175 (1988).
- E. H. Poindexter, "MOS Interface States: Overview and Physicochemical Perspective," *Semicond. Sci. Technol.* 4, 961 (1989).
- 67. C. J. Sofield and A. M. Stoneham, "Oxidation of Silicon: The VLSI Gate Dielectric?" *Semicond. Sci. Technol.* **10**, 215 (1995).
- 68. T. Hattori, "Chemical Structure of the SiO<sub>2</sub>/Si Interface," CRC Crit. Rev. Solid State Mater. Sci. 20, 339 (1995).
- 69. T. Engel, "The Interaction of Molecular and Atomic Oxygen with Si(100) and Si(111)," Surf. Sci. Rep. 18, 91 (1993).
- B. E. Deal, "Historic Perspectives of Silicon Oxidation," The Physics and Chemistry of SiO<sub>2</sub> and the Si-SiO<sub>2</sub> Interface, C. R. Helms and B. E. Deal, Eds., Plenum Press, New York, 1988, p. 5.
- 71. J. F. Conley and P. M. Lenahan, "A Review of Electron Spin Resonance Spectroscopy of Defects in Thin Films SiO<sub>2</sub> on Si," *The Physics and Chemistry of SiO<sub>2</sub> and the* Si-SiO<sub>2</sub> Interface—3, H. Z. Massoud, E. H. Poindexter, and C. R. Helms, Eds., The Electrochemical Society, Pennington, NJ, 1996, p. 214.
- M. Navi and S. T. Dunham, "Investigation of Boron Penetration Through Thin Gate Dielectrics Including Role of Nitrogen and Fluorine," *J. Electrochem. Soc.* 145, 2545 (1998).
- M. R. Frost and C. W. Magee, "Characterization of Nitrided SiO<sub>2</sub> Thin Films Using SIMS," *Appl. Surf. Sci.* 104/105, 379 (1996).
- H. C. Lu, E. P. Gusev, T. Gustafsson, E. Garfunkel, M. L. Green, D. Brasen, and L. C. Feldman, "High Resolution Ion Scattering Study of Silicon Oxynitridation," *Appl. Phys. Lett.* 69, 2713 (1996).
- E. P. Gusev, H. C. Lu, T. Gustafsson, and E. Garfunkel, "Silicon Oxidation and Oxynitridation in the Ultrathin Regime: Ion Scattering Studies," *Brazil. J. Phys.* 27, 302 (1997).
- 76. E. Garfunkel, E. P. Gusev, H. C. Lu, T. Gustafsson, and M. L. Green, "Medium Energy Ion Scattering Studies of Silicon Oxidation and Oxynitridation," Fundamental Aspects of Ultrathin Dielectrics on Si-based Devices, E. Garfunkel, E. P. Gusev, and A. Y. Vul', Eds., Kluwer Academic Publishers, Dordrecht, Netherlands, 1998, p. 39.
- 77. J. F. van der Veen, "Ion Beam Crystallography of Surfaces and Interfaces," Surf. Sci. Rep. 5, 199 (1985).
- E. P. Gusev, K. Morino, M. Hirose, and M. L. Green, "High Resolution Photoemission Study of Ultrathin Oxynitride Film," Proceedings of the American Vacuum Society Annual Meeting, San Jose, CA, 1997.
- A. Gupta, S. Toby, E. P. Gusev, H. C. Lu, Y. Li, M. L. Green, T. Gustafsson, and E. Garfunkel, "Nitrous Oxide Gas Phase Chemistry During Silicon Oxynitride Growth," *Progr. Surf. Sci.* 59, 103 (1998).
- M. L. Green, T. Sorsch, L. Feldman, W. N. Lennard, E. P. Gusev, E. Garfunkel, H. C. Lu, and T. Gustafsson, "Ultrathin SiO<sub>2</sub>N<sub>3</sub> by Rapid Thermal Heating of Silicon in N<sub>2</sub> at T = 760–1050°C," Appl. Phys. Lett. 71, 2978 (1997).
- 81. È. P. Gusev, M. L. Green, H. C. Lu, E. Garfunkel, T. Gustafsson, D. Brasen, and W. N. Lennard, "Nitrogen Engineering of Ultrathin Oxynitrides by a Thermal NO/O<sub>2</sub>/NO Process," *J. Appl. Phys.* **84**, 2980 (1998).
- S. Dimitrijev, D. Sweatman, and H. B. Harrison, "Model for Dielectric Growth on Silicon in a Nitrous Oxide Environment," *Appl. Phys. Lett.* 62, 1539 (1993).
- 83. B. Doyle, H. R. Soleimani, and A. Philipossian, "Simultaneous Growth of Different Thickness Gate Oxides in Silicon CMOS Processing," *IEEE Electron Device Lett.* **16**, 301 (1995).

- 84. C. T. Liu, E. J. Lloyd, Y. Ma, M. Du, R. L. Opila, and S. J. Hillenius, "High Performance 0.2 μm CMOS with 25 Å Gate Oxide Grown on Nitrogen Implanted Silicon," Technical Digest International Electron Devices Meeting, 1996, p. 499.
- R. C. DeMeo and T. P. Chow, "Thermal Oxidation Kinetics of (100) and (111) Silicon in N<sub>2</sub>O," *Appl. Phys. Lett.* 67, 500 (1995).
- A. E. T. Kuiper, H. G. Pomp, P. M. Asveld, W. A. Bik, and F. H. P. M. Habraken, "Nitrogen and Oxygen Incorporation During Thermal Processing of Si in N<sub>2</sub>O," Appl. Phys. Lett. 61, 1031 (1992).
- S. I. Raider, R. A. Gdula, and J. R. Petrak, "Nitrogen Reaction at the Si–SiO<sub>2</sub> Interface," *Appl. Phys. Lett.* 27, 150 (1975).
- 88. W. Ting, H. Hwang, J. Lee, and D. L. Kwong, "Growth Kinetics of Ultrathin SiO<sub>2</sub> Films in N<sub>2</sub>O," *J. Appl. Phys.* **70,** 1072 (1991).
- P. J. Tobin, Y. Okada, S. A. Ajuria, V. Lakhotia, W. A. Feil, and R. I. Hedge, "Furnace Formation of Silicon Oxynitride Thin Dielectrics in N<sub>2</sub>O," *J. Appl. Phys.* 75, 1811 (1994).
- N. Koyama, T. Endoh, H. Fukuda, and S. Nomura, "Growth Kinetics of Ultrathin Silicon Dioxide Films Formed by Oxidation in N<sub>2</sub>O," *J. Appl. Phys.* 79, 1464 (1996).
- 91. R. B. Fair, "Physical Models of Boron Diffusion in Ultrathin Gate Oxides," *J. Electrochem. Soc.* **144**, 708 (1997).
- K. A. Ellis and R. A. Buhrman, "Boron Diffusion in Silicon Oxides and Oxynitrides," *J. Electrochem. Soc.* 145, 2068 (1997).
- C. Tsamis, D. N. Kouvatsos, and D. Tsoukalas, "Influence of N<sub>2</sub>O Oxidation of Silicon on Point Defect Injection Kinetics in the High Temperature Regime," Appl. Phys. Lett. 69, 2725 (1996).
- 94. E. H. Poindexter, G. J. Gerardí, and D. J. Keeble, "Hydrogen Speciations in Electronic Silica," *The Physics and Chemistry of SiO<sub>2</sub> and the Si-SiO<sub>2</sub> Interface—3*, H. Z. Massoud, E. H. Poindexter, and C. R. Helms, Eds., The Electrochemical Society, Pennington, NJ, 1996, p. 172.
- 95. J. A. Aboaf, "Formation of 20–25 Å Thermal Oxide Films on Silicon at 950–1140°C," *J. Electrochem. Soc.* **118**, 1370 (1971).
- I. J. R. Baumvol, F. C. Stedile, J. J. Ganem, I. Trimaille, and S. Rigo, "Thermal Nitridation of SiO<sub>2</sub> with Ammonia," J. Electrochem. Soc. 143, 2938 (1996).
- I. J. R. Baumvol, F. C. Stedile, J. J. Ganem, I. Trimaille, and S. Rigo, "Nitrogen Transport During Rapid Thermal Growth of Silicon Oxynitride in N<sub>2</sub>O," *Appl. Phys. Lett.* 69, 2385 (1996).
- M. Revitz, S. I. Raider, and R. A. Gdula, "Effect of High-Temperature, Postoxidation Annealing on the Electrical Properties of the Si-SiO<sub>2</sub> Interface," *J. Vac. Sci. Technol.* 16, 345 (1979).
- Z. H. Lu, R. J. Hussey, M. J. Graham, R. Cao, and S. P. Tay, "Rapid Thermal N<sub>2</sub>O Oxynitride on Si(100)," J. Vac. Sci. Technol. B 14, 2882 (1996).
- 100. G. M. Rignanese, A. Pasquarello, J. C. Charlier, X. Gonze, and R. Car, "Nitrogen Incorporation at Si(001)-SiO<sub>2</sub> Interfaces: Relation Between N1s Core-Level Shifts and Microscopic Structure," *Phys. Rev. Lett.* 79, 5174 (1997).
- 101. E. Atanassova and A. Paskaleva, "Structural Changes in Thin SiO<sub>2</sub> on Si After RIE-like Nitrogen Plasma Action," Appl. Surf. Sci. 120, 306 (1997).
- 102. T. S. Chao, W. H. Chen, and T. F. Lei, "FTIR Study of Oxide Films Grown in Pure N<sub>2</sub>O," Jpn. J. Appl. Phys. 34, 2370 (1995).
- 103. E. A. Irene, Q. Liu, W. M. Paulson, P. J. Tobin, and R. I. Hedge, "Measurements of Nitrogen in Nitrided

- Oxides Using Spectroscopic Immersion Ellipsometry," J. Vac. Sci. Technol. B 14, 1697 (1996).
- 104. J. J. Ganem, G. Battistig, S. Rigo, and I. Trimaille, "A Study of the Initial Stages of the Oxidation of Silicon Using O<sup>18</sup> and RTP," *Appl. Surf. Sci.* 65/66, 647 (1993).
  105. I. J. R. Baumvol, F. C. Stedile, J. J. Ganem, I. Trimaille,
- 105. I. J. R. Baumvol, F. C. Stedile, J. J. Ganem, I. Trimaille and S. Rigo, "Thermal Nitridation of SiO<sub>2</sub> Films in Ammonia: The Role of Hydrogen," *J. Electrochem. Soc.* 143, 1426 (1996).
- 106. I. J. R. Baumvol, E. P. Gusev, F. C. Stedile, F. L. Freire, M. L. Green, and D. Brasen, "On the Behavior of Deuterium in Ultrathin SiO<sub>2</sub> Films upon Thermal Annealing," Appl. Phys. Lett. 72, 450 (1998).
- 107. R. M. Tromp, M. Copel, M. C. Reuter, M. Horn von Hoegen, J. Speidell, and R. Koudijs, "A New 2-D Particle Detector for a Toroidal Electrostatic Analyser," *Rev. Sci. Instrum.* 62, 2679 (1991).
- 108. H. C. Lu, E. P. Gusev, E. Garfunkel, and T. Gustafsson, "An Ion Scattering Study of the Interaction of Oxygen with Si(111): Surface Roughening and Oxide Growth," Surf. Sci. 341, 111 (1996).
- 109. J. Vrijmoeth, P. M. Zagwijn, J. W. M. Frenken, and J. F. van der Veen, "Monolayer Resolution in Medium-Energy Ion-Scattering Experiments on the NiSi<sub>2</sub>(111) Surface," *Phys. Rev. Lett.* 67, 1134 (1991).
- 110. F. Besenbacher, J. U. Andersen, and E. Bonderup, "Straggling in Energy Loss of Energetic Hydrogen and Helium Ions," *Nucl. Instr. Meth.* **168**, 1 (1980).
- 111. E. P. Gusev, H. C. Lu, T. Gustafsson, and E. Garfunkel, "The Growth Mechanism of Thin Silicon Oxide Films on Si(100) Studied by Medium Energy Ion Scattering," *Phys. Rev. B* **52**, 1759 (1995).
- 112. H. C. Lu, T. Gustafsson, E. P. Gusev, and E. Garfunkel, "An Isotopic Labeling Study of the Growth of Thin Oxide Films on Si(100)," *Appl. Phys. Lett.* **67**, 1742 (1995).
- 113. M. Copel and R. M. Tromp, "Hydrogen Coverage Dependence of Si(100) Homoepitaxy," *Phys. Rev. Lett.* **72**, 1236 (1994).
- 114. M. Copel and R. M. Tromp, "Elastic Recoil Detection for MEIS," *Rev. Sci. Instrum.* **64,** 3147 (1993).
- 115. E. P. Gusev, H. C. Lu, T. Gustafsson, and E. Garfunkel, "On the Mechanism of Ultrathin Silicon Oxide Film Growth During Thermal Oxidation," *Interface Control of Electrical, Chemical, and Mechanical Properties*, S. P. Murarka, K. Rose, T. Ohmi, and T. Seidel, Eds., MRS Vol. 318, 1994, p. 69.
- E. P. Gusev, H. C. Lu, T. Gustafsson, and E. Garfunkel, "Initial Oxidation of Silicon: New Ion Scattering Results in the Ultrathin Regime," *Appl. Surf. Sci.* 104/105, 329 (1996).
- 117. E. P. Gusev, H. C. Lu, T. Gustafsson, and E. Garfunkel, "New Features of Silicon Oxidation in the Ultrathin Regime: An Ion Scattering Study," *The Physics and Chemistry of SiO<sub>2</sub> and the Si-SiO<sub>2</sub> Interface—3*, H. Z. Massoud, E. H. Poindexter, and C. R. Helms, Eds., The Electrochemical Society, Pennington, NJ, 1996, p. 49.
- S. I. Raider and R. Flitsch, "X-ray Photoelectron Spectroscopy of SiO<sub>2</sub>-Si Interfacial Regions: Ultrathin Oxide Films," *IBM J. Res. Develop.* 22, 294 (1978).
- 119. F. J. Grunthaner and P. J. Grunthaner, "Chemical and Electronic Structure of the SiO<sub>2</sub>/Si Interface," *Mater. Sci. Rep.* 1, 65 (1986).
- 120. F. G. Himpsel, "Electronic Structure of Semiconductor Interfaces," Surf. Sci. 299/300, 525 (1994).
- 121. M. M. Banaszak-Holl, S. Lee, and F. R. McFeely, "Core-Level Photoemission and the Structure of the Si/SiO<sub>2</sub> Interface," *Appl. Phys. Lett.* **65**, 1097 (1994).
- 122. S. R. Kaluri and D. W. Hess, "Nitrogen Incorporation in Thin Oxides by Constant Current N,O Plasma

- Anodization of Silicon and N<sub>2</sub> Plasma Nitridation of Silicon Oxides," *Appl. Phys. Lett.* **69**, 1053 (1996).
- 123. Z. H. Lu, J. P. McCaffrey, B. Brar, G. D. Wilk, R. M. Wallace, L. C. Feldman, and S. P. Tay, "SiO<sub>2</sub> Film Thickness Metrology by X-Ray Photoelectron Spectroscopy," *Appl. Phys. Lett.* 71, 2764 (1997).
- 124. F. J. Himpsel, F. R. McFeely, A. Taleb-Ibrahimi, J. A. Yarmoff, and G. Hollinger, "Microscopic Structure of the SiO<sub>3</sub>/Si Interface," *Phys. Rev. B* **38**, 6084 (1988).
- 125. J. I. Dadap, X. F. Hu, M. H. Anderson, M. C. Downer, J. K. Lowell, and O. A. Aktsipetrov, "Optical Second-Harmonic Electroreflectance Spectroscopy of a Si(001) Metal-Oxide-Semiconductor Structure," *Phys. Rev. B* 53, R7607 (1996).
- 126. C. Meyer, G. Lupke, U. Emmerichs, F. Wolter, H. Kurz, C. H. Bjorkman, and G. Lucovsky, "Electronic Transitions at Si(111)/SiO<sub>2</sub> and Si(111)/Si<sub>3</sub>N<sub>4</sub> Interfaces Studied by Optical Second-Harmonic Spectroscopy," *Phys. Rev. Lett.* 74, 3001 (1995).
- 127. Y. Okada, P. J. Tobin, and S. A. Ajuria, "Furnace Grown Silicon Oxynitrides Using NO," *IEEE Trans. Electron Devices* **41**, 1608 (1994).
- 128. N. S. Saks, D. I. Ma, and W. B. Fowler, "Nitrogen Depletion During Oxidation in N<sub>2</sub>O," Appl. Phys. Lett. 67, 374 (1995).
- 129. M. D. Wiggins, R. J. Baird, and P. Wynblatt, "Thermal Nitridation of Si(111) by Nitric Oxide," *J. Vac. Sci. Technol.* **18**, 965 (1981).
- 130. E. H. Poindexter and W. L. Warren, "Paramagnetic Point Defects in Amorphous Thin Films of SiO<sub>2</sub> and Si<sub>3</sub>N<sub>4</sub>: Updates and Additions," *J. Electrochem. Soc.* 142, 2508 (1995).
- 131. B. E. Deal and A. S. Grove, "General Relationship for the Thermal Oxidation of Silicon," *J. Appl. Phys.* **36**, 3770 (1965).
- 132. F. Rochet, S. Rigo, M. Froment, C. d'Anterroches,
  C. Maillot, H. Roulet, and G. Dufour, "The Thermal Oxidation of Silicon: The Special Case of the Growth of Very Thin Films," *Adv. Phys.* 35, 339 (1986).
  133. I. Trimaille and S. Rigo, "Use of <sup>18</sup>O Isotopic Labeling
- 133. I. Trimaille and S. Rigo, "Use of "O Isotopic Labeling to Study Thermal Dry Oxidation of Silicon as a Function of Temperature and Pressure," *Appl. Surf. Sci.* **39**, 65 (1989).
- 134. N. F. Mott, S. Rigo, F. Rochet, and A. M. Stoneham, "Oxidation of Silicon," *Phil. Mag. B* **60**, 189 (1989).
- 135. M. J. Hartig and P. J. Tobin, "A Model for the Gas-Phase Chemistry Occurring in a Furnace N<sub>2</sub>O Oxynitride Process," J. Electrochem. Soc. 143, 1753 (1996).
- 136. Y. Ishikawa, Y. Takagi, and I. Nakamichi, "Low-Temperature Thermal Oxidation of Silicon in N<sub>2</sub>O by UV-Radiation," *Jpn. J. Appl. Phys.* 28, L1453 (1989).
  137. A. Namiki and K. Tanimoto, "XPS Study of the Early
- 137. A. Namiki and K. Tanimoto, "XPS Study of the Early Stages of Oxidation of Si(100) by Atomic Oxygen," *Surf. Sci.* **222**, 530 (1989).
- 138. T. Y. Chu, W. T. Ting, J. Ahn, and D. L. Kwong, "Thickness and Compositional Non-uniformities of Ultrathin Oxides Grown by Thermal Oxidation of Silicon in N<sub>2</sub>O," *J. Electrochem. Soc.* **138**, L13 (1991).
- 139. K. A. Ellis and R. A. Buhrman, "Nitrous Oxide (N<sub>2</sub>O) Processing for Silicon Oxynitride Gate Dielectrics," *IBM J. Res. Develop.* 43, 287 (1999, this issue).
- 140. E. Briner, C. Meiner, and A. Rothen, "Recherches sur la Decomposition Thermique du Protoxyde et de l'Oxyde d'Azote," J. Chim. Phys. 23, 609 (1926).
- 141. NIST Chemical Kinetics Database, 1994.
- 142. S. Singhvi and C. G. Takoudis, "Growth Kinetics of Furnace Silicon Oxynitridation in Nitrous Oxide Ambients," J. Appl. Phys. 82, 442 (1997).
- 143. M. L. Green, D. Brasen, B. J. Sapjeta, T. W. Sorsch, G. Timp, W. N. Lennard, E. P. Gusev, H. C. Lu, E. Garfunkel, and T. Gustafsson, "Growth of Silicon

- Oxynitride Films in NO-O<sub>2</sub> Gas Mixtures," Semiconductor Silicon 1998, R. H. Huff, U. Gosele, and H. Tsuya, Eds., The Electrochemical Society, Pennington, NJ, 1998, p. 745.
- 144. E. G. Keim, L. Wolterbeek, and A. van Silfhout, "Adsorption of Atomic Oxygen (N<sub>2</sub>O) on a Clean Si(100) Surface and Its Influence on the Surface State Density: A Comparison with O<sub>2</sub>," Surf. Sci. 180, 565 (1987).
- 145. N. Gonon, A. Gagnaire, D. Barbier, and A. Glachant, "Growth and Structure of Rapid Thermal Silicon Oxides and Nitrides Studied by Spectroellipsometry and Auger Electron Spectroscopy," J. Appl. Phys. 76, 5242 (1994).
- 146. T. S. Chao and T. F. Lei, "Crossover Phenomenon in Oxidation Rates of the (110) and (111) Orientations of Silicon in N<sub>2</sub>O," *J. Electrochem. Soc.* **142**, L34 (1995).
- 147. K. A. Ellis and R. A. Buhrman, "The Removal of Nitrogen During Boron In-Diffusion in Silicon Gate Oxynitrides," Appl. Phys. Lett. 70, 545 (1997).
- 148. T. Ito, D. Kitayama, and H. Ikoma, "Silicon Oxynitridation with Inductively Coupled Oxygen Nitrogen Mixed Plasma," *Jpn. J. Appl. Phys.* 36, 612 (1997).
- 149. R. P. Vasquez, M. H. Hecht, F. J. Grunthaner, and M. L. Naiman, "X-ray Photoelectron Spectroscopy Study of the Chemical Structure of Thermally Nitrided SiO<sub>2</sub>," Appl. Phys. Lett. 44, 969 (1984).
- 150. T. Hori, H. Iwasaki, and K. Tsuji, *IEEE Trans. Electron Devices* ED-35, 904 (1988).
- 151. C. Maillot, H. Roulet, and G. Dufour, "Thermal Nitridation of Silicon: An XPS and LEED Investigation," J. Vac. Sci. Technol. B 2, 316 (1984).
- 152. C. H. F. Peden, J. W. Rogers, N. D. Shinn, K. B. Kidd, and K. L. Tsang, "Thermally Grown Si<sub>3</sub>N<sub>4</sub> Thin Films on Si(100): Surface and Interfacial Composition," *Phys. Rev. B* 47, 15,622 (1993).
- 153. A. A. Saranin, O. L. Tarasova, V. G. Kotljar, E. A. Khramtsova, and V. G. Lifshits, "Thermal Nitridation of the Si(110) by NH<sub>3</sub>: LEED and AES Study," *Surf. Sci.* 331–333, 458 (1995).
- 154. J. Watanabe and M. Hanabusa, "Photochemical Vapor Deposition of Silicon Oxynitride Films by Deuterium Lamp," J. Mater. Res. 4, 882 (1989).
- Y. Saito, "Oxynitridation of Silicon by Remote-Plasma Excited Nitrogen and Oxygen," Appl. Phys. Lett. 68, 800 (1996).
- 156. C. Lin, A. I. Chou, P. Choudhury, J. C. Lee, K. Kumar, B. Doyle, and H. R. Soleimani, "Reliability of Gate Oxide Grown on Nitrogen-Implanted Si Substrates," *Appl. Phys. Lett.* 69, 3701 (1996).
- 157. S. M. George, O. Sneh, and J. D. Way, "Atomic Layer Controlled Deposition of SiO<sub>2</sub> and Al<sub>2</sub>O<sub>3</sub> Using ABAB... Binary Reaction Sequence Chemistry," *Appl. Surf. Sci.* 82/83, 460 (1994).
- T. Suntola, "Atomic Layer Epitaxy," *Mater. Sci. Rep.* 4, 261 (1989).

Received March 1, 1998; accepted for publication October 21, 1998

Evgeni P. Gusev IBM Research Division, Thomas J. Watson Research Center and Semiconductor Research and Development Center, P.O. Box 218, Yorktown Heights, New York 10598 (gusev@us.ibm.com). Dr. Gusev received his M.S. degree in molecular physics (1988) and his Ph.D. in solid-state physics (1992) from the Moscow Engineering Physics Institute (MEPhI). From 1988 to 1992, he worked at MEPhI as a Research Associate. From 1993 to 1998, he was a Research Associate and then Research Assistant Professor at the Laboratory for Surface Modification at Rutgers University. In 1997, he was a Visiting Professor at the Research Center for Nanodevices and Systems, Hiroshima University, Japan. Dr. Gusev is currently a member of the Advanced Gate Dielectrics group at the IBM Thomas J. Watson Research Center. His research areas include experimental and theoretical aspects of surface and thin-film science, materials science, semiconductor physics, and physical and chemical kinetics. Dr. Gusev is a member of the American Vacuum Society, the American Physical Society, and the Electrochemical Society.

Hsu-Chang Lu Department of Physics and Laboratory for Surface Modification, Rutgers University, Piscataway, New Jersey 08854 (hclu@physics.rutgers.edu). Dr. Lu received his B.S. degree in physics in 1988 from the National Taiwan University in Taipei, Taiwan. He received his M.S. and Ph.D. degrees in physics at Rutgers University in 1995 and 1997, respectively. He has been a postdoctoral research associate at Rutgers since 1997, working on ultrathin-gate dielectrics using medium-energy ion scattering.

**Eric L. Garfunkel** Department of Chemistry and Laboratory for Surface Modification, Rutgers University, Piscataway, New Jersey 08854 (garf@rutchem.rutgers.edu). Prof. Garfunkel received his B.S. degree from Haverford College in 1978 and his Ph.D. in 1983 at U.C. Berkeley with Prof. G. A. Somorjai. From 1983 to 1984 he worked in France as an NSF-CNRS Exchange Scholar at the University of Paris-Sud, Orsay, and in China as an NAS Fellow at Fudan University. Since September 1984, he has worked as an Assistant, Associate, and now full Professor of Chemistry at Rutgers University. He has also had visiting positions at the Ruhr Universitat (Bochum), at the BESSY synchrotron facility (Berlin), at the Univ. of Paris-VII, and at the Instituto Degli Studio (Florence, Italy). At Rutgers, Prof. Garfunkel's research has included studies of molecular and metal adsorption and reaction, thin-film growth, interface structure, and oxidation. He uses electron spectroscopy, ion scattering, scanning probe microscopies (STM and AFM), and other surface science and thin-film methods. One project involves studies of silicon oxidation, oxynitridation, and the growth of higher-dielectricconstant materials for gate dielectric applications. He is interested in questions of growth mechanism, interface and film structure, and device properties. Other projects include structural and thermochemical aspects of metallization, and studies of the polymer-metal interface.

**Torgny Gustafsson** Department of Physics and Laboratory for Surface Modification, Rutgers University, Piscataway, New Jersey 08854 (gustaf@physics.rutgers.edu). Dr. Gustafsson received M.Sc. and Ph.D. degrees from Chalmers University of Technology, Göteborg, Sweden, in 1970 and 1973. He was a Research Associate, Assistant Professor, Associate Professor, and Professor of Physics at the University of Pennsylvania from 1974 to 1987. Since 1987, he has been a

Professor (II) of Physics at Rutgers University. He has held visiting positions at the University of Wisconsin (1977), Stanford University and Xerox PARC (1978), Chalmers University (1979), and the FOM Institute, Amsterdam (1985). Dr. Gustafsson was awarded The Nottingham Prize (Physical Electronics Conference, 1974) and an Alfred P. Sloan Foundation Fellowship (1978–1982). He is a Fellow of the American Physical Society.

Martin L. Green Bell Laboratories/Lucent Technologies, Murray Hill, New Jersey 07974 (mlg@lucent.com). Dr. Green received B.S. and M.S. degrees in metallurgy in 1970 and 1972, respectively, from the Polytechnic Institute of Brooklyn. He was the Climax Molybdenum Fellow at MIT from 1974 to 1978, receiving his Ph.D. in materials science there in 1978. In 1977, he was a Kurtz Memorial Fellow at the Technion in Israel. He has been with Bell Laboratories since 1978, working in the fields of phase transformations, magnetic materials, ordered alloys, CVD metal films for ULSI, SiGe heteroepitaxy, and, most recently, ultrathin-gate dielectrics. He is a member of the Metallurgical Society, the Materials Research Society, and the Electrochemical Society.